

**Study, Design And Analysis Of H₂ Gas Actuated Pneumatic Artificial Muscle
Using Metal Hydride as Gas Storage Medium**

by

Shasindran Shanmugam

Dissertation submitted in partial fulfilment of

the requirements for the

Bachelor of Engineering (Hons)

(Mechanical Engineering)

MAY 2011

Universiti Teknologi PETRONAS

Bandar Seri Iskandar

31750 Tronoh

Perak Darul Ridzuan

CERTIFICATION OF APPROVAL

**Study, Design And Analysis Of H₂ Gas Actuated Pneumatic Artificial Muscle
Using Metal Hydride as Gas Storage Medium**

by

Shasindran Shanmugam

A project dissertation submitted to the
Mechanical Engineering Programme
Universiti Teknologi PETRONAS
in partial fulfilment of the requirement for the
BACHELOR OF ENGINEERING (Hons)
(MECHANICAL ENGINEERING)

Approved by,



(Prof. Dr. T. Nagarajan)

Dr T. Nagarajan
Professor
Mechanical Engineering Department
Universiti Teknologi PETRONAS


UNIVERSITI TEKNOLOGI PETRONAS

TRONOH, PERAK

May 2011

CERTIFICATION OF ORIGINALITY

This is to certify that I am responsible for the work submitted in this project, that the original work is my own except as specified in the references and acknowledgements, and that the original work contained herein have not been undertaken or done by unspecified sources or persons.



SHASINDRAN SHANMUGAM

ACKNOWLEDGMENT

I would like to take this opportunity to dedicate my utmost appreciation to those who have aided me with the completion of the project. First of all, I would like to thank Prof. Dr. T. Nagarajan for giving me the opportunity to carry out this project and gave the generative ideas regarding the projects and initiated the objectives in order to make the project meaningful. Special thanks go to Prof. Dr. Vijay Raghavan and Ir. AP Mohd Amin Bin Abd Majid, who have given me all the guidance that I needed in order to carry out the project. I also would like to thank my parents for the support given for the completion of the project, and not forgetting the almighty God who has assisted me in every part of my life too. Thank You.

ABSTRACT

This report contains all the necessary information gathered from literature review and other technical sources to carry out this project. The aim of this project is to study, design and analyse H₂ Gas Actuated Pneumatic Artificial Muscle (PAM) using Metal Hydride as the hydrogen storage medium. Studies and design on this project is intended to assist disabled and paralysed people physically. This project portrays an actuation system to idealise a more flexible mechanical system, which has longer serving-life, ability to deliver high force-to-weight ratio, and less mechanical wear compared to pneumatic piston cylinder actuator. The research discusses the ability, type, and quantity of metal hydride to store and release hydrogen to actuate the PAM. It also discusses the maximum amount of hydrogen gas that is needed for the actuation and hydrogen storage for 30mm diameter of BPAM. The validity of this actuation in the aspect of contraction/expansion is modeled with Finite Element ANSYS simulation for 3 diameters that are OD= 10mm, 20mm and 30mm. Design of functional prototype of prosthesis arm is shown with Catia V5R12 3D modeling. This paper defines PAM with a diameter of 30mm and length of 140mm is capable to produce 10.20% contraction with only 1.2g of sodium aluminium hydride. It gives 10.20% axial contraction i.e. from 140mm to 125.71mm that is more than PAM with OD of 10mm and 20mm.

TABLE OF CONTENTS

CERTIFICATION		ii
ACKNOWLEDGEMENT		iv
ABSTRACT		v
CHAPTER 1:	INTRODUCTION	1
	1.1 Background of Study	1
	1.2 Problem Statement	1
	1.3 Objective	3
	1.4 Scope of Study	3
CHAPTER 2:	LITERATURE REVIEW	4
	2.1 Paralyzed Patient Statistics	4
	2.2 Braided Pneumatic Artificial Muscle	5
	2.3 Metal Hydride & Hydrogen Storage Systems	7
	2.4 Isentropic Processes	10
	2.5 Ideal Gas Law	13
	2.6 Relationship Volumetric H ₂ density vs Gravimetric H ₂ Density	14
	2.7 Natural Limb Structure & Artificial Limb Structure	16
CHAPTER 3:	METHODOLOGY	18
	3.1 Flow of Tasks	18
	3.2 Project Planning, Work Done & Gantt Chart	20
CHAPTER 4:	RESULT AND DISCUSSION	
	4.1 Material Selection	21
	4.2 Analyses of volume and pressure of H ₂ needed for 3 varied diameters	23
	4.3 Required Mass of Sodium Aluminium Hydride, NaAlH ₄	24
	4.4 Artificial Arm (BPAM-Load System)	26
	4.5 Simulation of BPAM	28
CHAPTER 5:	CONCLUSION AND RECOMMENDATION	
	5.1 CONCLUSION	40
	5.2 RECOMMENDATIONS	40
REFERENCE		41
APPENDICES		43

LIST OF FIGURES

Figure 1.1	Storage method and its volume capacity to store 1kg of hydrogen gas	2
Figure 2.1	Pie chart of paralysis causes	4
Figure 2.2	Concept diagram of BPAM operation	5
Figure 2.3	BPAMs consist of a closed rubber tubing (with an inlet for gas) sheathed in a braided sleeve	6
Figure 2.4	Braided sleeve (a) and unrolled sleeve (b)	6
Figure 2.5	Operating principle of PAM	7
Figure 2.6	Simplified system diagram	8
Figure 2.7	Schematic diagram of a metal hydride driven braided artificial pneumatic muscle	9
Figure 2.8	(a) and (b) Reactor containment unit design showing metal hydride pellets enclosed in reactor unit chambers, (c) actual sealed containment unit, and (d) metal hydride pellets	10
Figure 2.9	Schematic of the metal hydride hydrogen storage vessel	10
Figure 2.10	Relationship of stored hydrogen per mass and per volume in volumetric H ₂ density vs gravimetric H ₂ density graph	14
Figure 2.11	The calculated volume and weight of hydrogen storage for mobile application	15
Figure 2.12	The biceps muscle in human arm	16
Figure 2.13	The bone structure in upper limbs	17
Figure 3.1	Task flow for metal hydride system	18
Figure 3.2	Task flow for PAM simulation i.e. radial expansion and axial contraction	19
Figure 4.1	Stability of Hydrides: Van't Hoff Plot	22
Figure 4.2	NaAlH ₄ & its relationship of stored hydrogen per mass and per volume in volumetric H ₂ density vs gravimetric H ₂ density graph	25
Figure 4.3	Artificial arm	27
Figure 4.4	Hydride container	28
Figure 4.5	Geometry for L1, D1	28

Figure 4.6	Total deformation for L1, D1	29
Figure 4.7	Directional deformation along X axis.	29
Figure 4.8	Directional Deformation along Y axis	29
Figure 4.9	Directional Deformation along Z axis	29
Figure 4.10	Values of bands along X axis	30
Figure 4.11	Values of bands along Y axis	30
Figure 4.12	Graphical representation of the iteration results, OD=30mm.	33
Figure 4.13	Linear static FEA results	33
Figure 4.14	Graphical representation of the iteration results, OD=20mm.	35
Figure 4.15	Graphical representation of the iteration results, OD=10mm.	39

LIST OF TABLES

Table 3.1	Gantt chart of Semester 1 & 2.	20
Table 4.1	Isentropic process analyses with Pressure change from 1 to 6 bars	23
Table 4.2	Mass & Volume of Hydride Required	25
Table 4.3	Simulation and iteration results for L_i , D_i and percentage of contraction, 30mm.	32
Table 4.4	Simulation and iteration results for L_i , D_i and percentage of contraction, 20mm	34
Table 4.5	Simulation and iteration results for L_i , D_i and percentage of contraction, 10mm	37

CHAPTER 1

INTRODUCTION

1.1 Background of Study

Nowadays, the demand for research in prosthesis limbs and flexible actuator has risen to a significant amount [5]. The demand rises as amputation procedures increase on diabetics' patients, loss of limbs to accidents, gangrene and smoking. Prosthetic limbs are also widely used for the disabled. Doctors usually recommend the use of rigid plastic prosthetics to the disabled and affected people. This causes discomfort to the patients in a long run. Thus, creates health complications due to the rigid limbs. It restricts mobility for the affected people and also, the paralysed. Consequently, causes physiological problems after long term usage. Hence, a better model of movable or actuated prosthetic limbs will be able to assist them to enhance their mobility; and a research on actuated limbs is very much needed indeed.

1.2 Problem Statement

Advancement in actuation system forces engineers to idealise a more flexible mechanical system, which has longer serving-life, ability to deliver high force-to-weight ratio, and less mechanical wear compared to pneumatic piston cylinder system[1], [10]. Pneumatic cylinders are heavy because it is comprised of a lot of mechanical parts [7]. The components must be maintained regularly for good performance. Those characters of pneumatic cylinders are disadvantage for artificial limb actuation for humans. It is not feasible for disabled person to service regularly. Progression in this sector is foreseen to assist disabled and paralysed people. One of the possible innovations is Braided Pneumatic Artificial Muscle (BPAM). The BPAM actuated by H_2 gas is hoped to develop prosthesis limb technology for human beings and robotic industry [2].

On the other hand, a suitable hydrogen-supplying storage is needed to power the actuation system. Current storage systems are less mobile, heavy and most have very low H₂ storage capacity. Hence, it is crucial to upgrade or replace existing hydrogen-supplying storages – liquid hydrogen gas storage, hydride storage, and cryo-adsorbed gas storage – with a type of metal hydride that is a better alternative to current hydrogen storage capacity [11], [12], [13], [16].

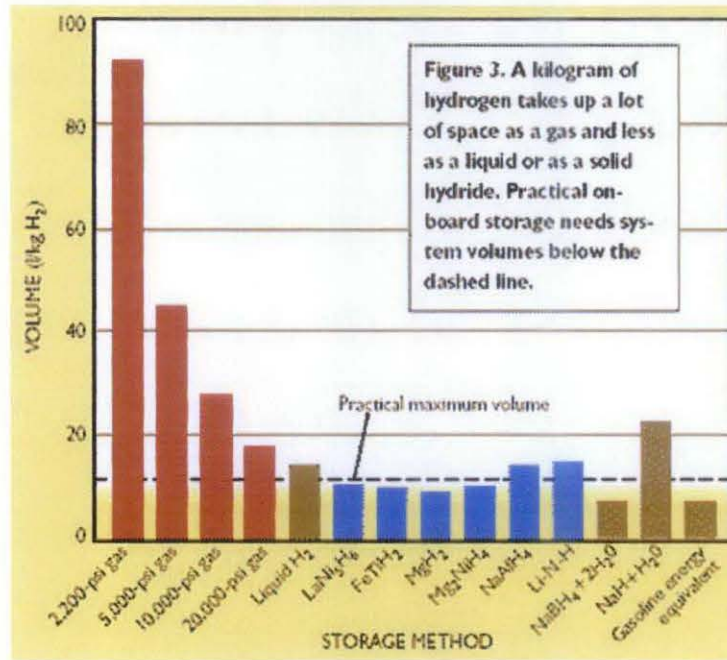


Figure 1.1: Shows the storage method and its volume capacity to store 1kg of hydrogen gas [11]

Current conventional methods of storage that are widely used are compressed hydrogen gas tanks and liquid hydrogen gas tanks. However, the storage volume that is needed for 1kg of hydrogen is relatively high compared to hydrides. For example, compressed gas tanks and liquid hydrogen tanks need more than 10L/kg H₂ whereas other options can store 1kg of hydrogen gas in less than 10L/kg H₂. The figure indicates there are other options that can be used as an alternative. The alternative may be an option to replace current storage methods after weighing its advantage and disadvantage to store hydrogen in given situation.

1.3 Objective & Scope of Study

The aim of this project is to study, design and analyse **H₂ Gas Actuated Pneumatic Artificial Muscle by Metal Hydride**. Studies and design on this project is intended to assist disabled and paralysed people physically. Where, the actuation performs contraction and extension of the pneumatic artificial muscles. Hence, would be very helpful for concerned patients and surgeons.

The objectives that have to be achieved in this project are:

1. Studies on the properties, material selection to select proper metal hydride that can absorb and release H₂ gas for the pneumatic actuation when cooled or heated.
2. Analysis on the volume and pressure of H₂ needed for the expansion and contraction of BPAM.
3. Determine the quantity of metal hydride.
4. Design artificial arm and metal hydride system.
5. Analyse the BPAM actuation through ANSYS simulation for OD=10mm, 20mm and 30mm and compare it.

The scope of my studies includes chemical, materials, mechanical and electrical field. Chemical and thermodynamics studies are applied to know the behaviour and properties of hydrogen gas at high temperature and high compression pressure. Material selection guides to choose the suitable type of metal hydride for desired operation temperature and volume output. While, mechanical knowledge is applied to design proper hydride containment and mechanism of BPAM system, whereas, the design of mechatronics control system is done with electrical knowledge.

The breakdown of this scope is as shown: -

Task	Related Scope and Software
Material selection	Material Science
Analysis on the volume and pressure of H ₂ needed	Chemistry and Thermodynamics of compressible H ₂ gas.
Expansion & Contraction of BPAM	Simulation with ANSYS software
Design of arm and hydride container	Draft with CATIA software

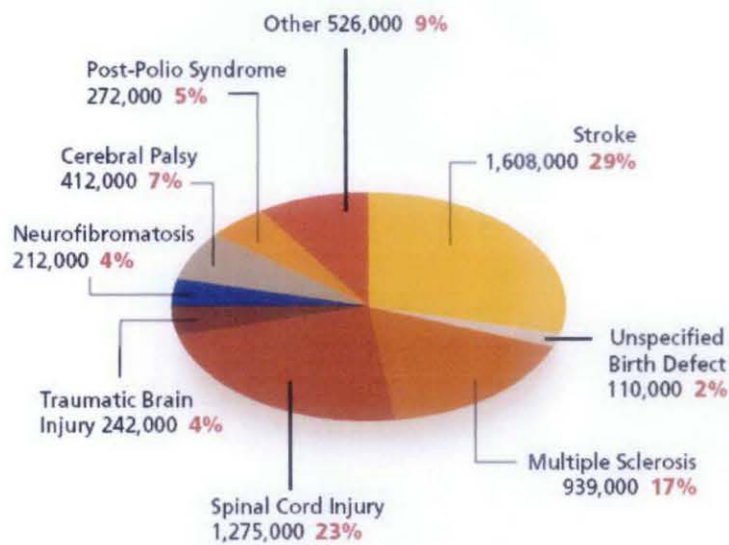
CHAPTER 2

LITERATURE REVIEW

This project is idealised to assist disabled and paralysed people all over the world. From the facts that were analysed from reliable sources; it shows that there are very large number of disabled or paralysed people. Although, there isn't sufficient data about the numbers of paralysed/ disabled in the world and Malaysia, United States' data is deemed to be relevant to show the statistics of people who will need the BPAM [5].

2.1 Paralysed Patient Statistics

Causes of Paralysis⁷
N= 5,596,000



Degree of Difficulty in Moving

- 36% of those who reported being paralyzed said they had "a lot of difficulty" in moving; 29% said "some difficulty"; 17% said "a little difficulty"; and 16% said they were "completely unable to move."
- 35% of those who reported being paralyzed due to a spinal cord injury said they had "a lot of difficulty" in moving; 29% percent said they had "some difficulty"; 20% said they had "a little difficulty"; and 13% were "completely unable" to move.

Figure 2.1: Pie chart of paralysis causes [5]

The figure that is picked from a trusted body in America shows that a large number of people ($N=5596000$) will need assistance in their physical movement. Thus, this project would provide a prototype that shall benefit them.

2.2 Braided Pneumatic Artificial Muscle

BPAM is fluid actuator that is actuated by water, nitrogen gas, or H_2 gas. The picture below shows the sample of BPAM:-

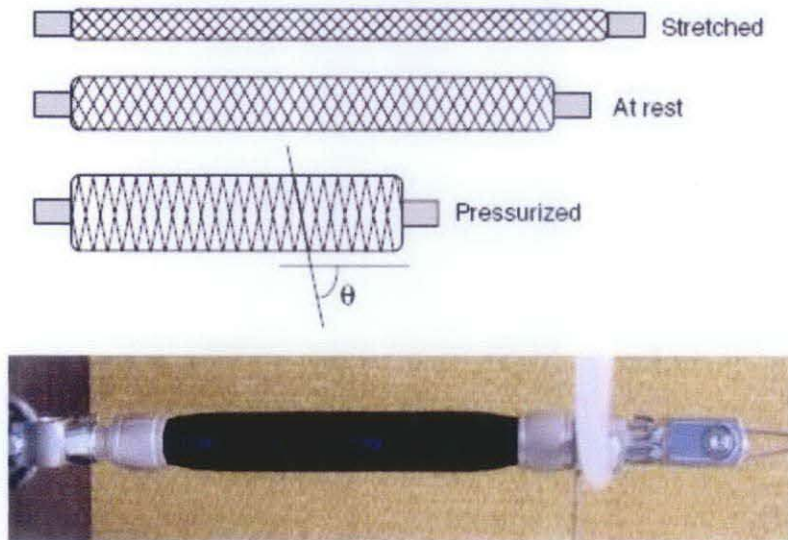


Figure 2.2: (top) Concept diagram of BPAM operation, where θ is the braid angle of the outer sleeve; (bottom) air pressure input to a Festo BPAM [10].

BPAMs consist of a closed rubber tubing (with an inlet for gas) sheathed in a braided sleeve as shown in Figure 2.3 [3]. As gas pressure is applied to the rubber tubing, it expands radially against the braided shell [14]. The braid angle of the shell increases. The muscle contracts in the axial direction producing the actuation displacement and force (when loaded) as shown in Figure 2.2.

The BPAM used in this diagram is from Festo [10, 23]. This particular BPAM uses the braiding that controls the actuation and that is made of strong aramid fibers embedded in a rubber chloroprene membrane, potentially reducing the friction caused by the rubbing of the braided sleeve in the BPAM design, and creating a more

durable and longer lasting fluidic muscle with nearly zero leakage. The entire weight of the Festo BPAM is 61.9 g. The end caps are machined from galvanized steel.

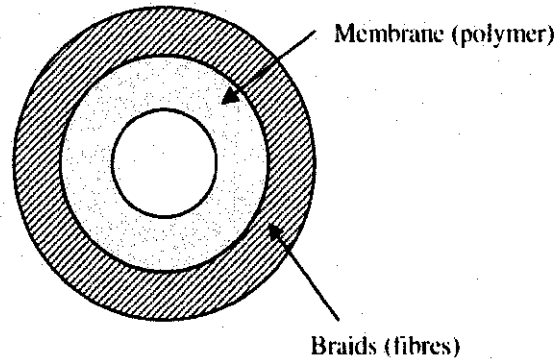


Figure 2.3: BPAMs consist of a closed rubber tubing (with an inlet for gas) sheathed in a braided sleeve [3].

Braided sleeve gives a special characteristic to the contraction of BPAM. The braided sleeve is characterized by braid angle. It is a manipulative variable that affects overall contraction of BPAM when pressure is applied to it. The contractile range of the actuator is the difference between the length of the actuator at the minimum and maximum braid angles [3]. Braided sleeve is as shown in the following Figure 2.4.

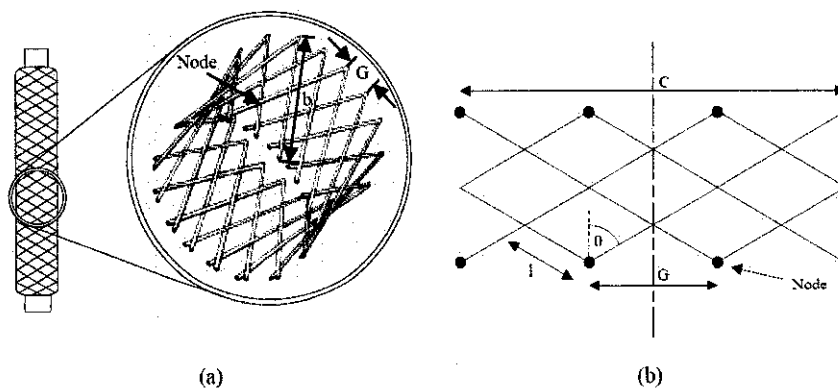


Figure 2.4: Braided sleeve (a) and unrolled sleeve (b) [24].

The effect of contraction that is caused by braided sleeve while pressure is applied can be seen in Figure 2.5. The diagram shows that the contraction is able to result in change of displacement. It proves BPAM expands radially against the braided shell and applies pulling force to the load [4, 8, 9]. The expansion is achievable by using any type of fluid like water, nitrogen gas, or H_2 gas.



Figure 2.5: Operating principle of PAM. Powered by compressed gas, artificial muscle actuator contracts lengthwise when expanded radially and convert the radial expansive force into axial contractile force [6].

2.3 Metal Hydride & Hydrogen Storage Systems

Compressed gaseous storage is widely used because of its familiarity and conceptual simplicity. The major difficulty with compressed hydrogen is its storage volume as referred to Figure 1.1. High-pressure tanks are complex structures containing multiple layers for hydrogen confinement, rupture strength, and impact resistance. Furthermore, the tank must be cylindrical or near cylindrical in shape, which seriously limits the options for tank placement/ mobility [11]. High-pressure storage is most appealing for large vehicles, such as buses, which have more available space—on the roof, for example but not for artificial muscle and limb.

Other than that, conventional liquid-hydrogen storage is currently being used in some areas like automobile. Here, the volumetric situation is somewhat improved compared to compressed gas because liquid hydrogen occupies about 14 l/kg (10 MJ/l, hydrogen basis). But hydrogen vaporizes at $-253\text{ }^{\circ}\text{C}$, which necessitates an exotic superinsulated cryogenic tank. Inevitably, heat leaking into the tank will produce serious boil-off, and the tank will begin to empty itself in days in un-used application.

Solid-hydride storage is considered a breakthrough in advanced hybrid materials which can store a large amount of hydrogen gas. Metal hydrides are extremely porous metals that lock onto and hold hydrogen gas at lower pressures and temperatures than is possible with cold and highly compressed pure hydrogen gas

[2]. Volume is not the primary issue (Figure 1.1) for metal hydride hydrogen storage. In fact, many hydrides, store more hydrogen per unit volume than does liquid hydrogen. Solid-hydride storage materials then would release hydrogen gas under suitable conditions of temperature and hydrogen pressure (generally 2–5 bar).

Thus, to minimize the size of BPAM and artificial limb system, normal fluid storage is not used to supply necessary pressure to it. It is mainly because large tanks are used as the storage mediums [1]. Since metal hydrides can store very large volume of H₂ gas, it is preferred as the best available storage option [10-13].

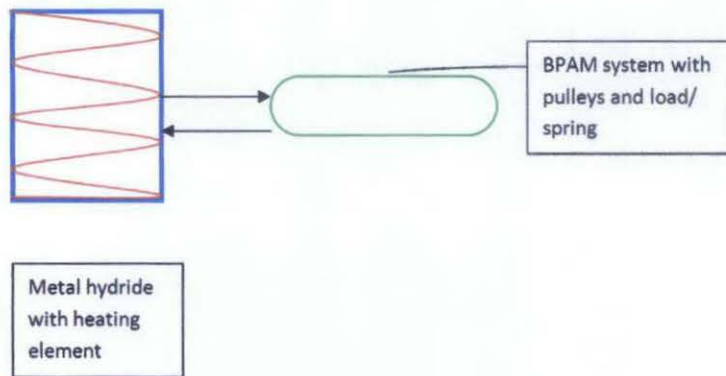


Figure 2.6: Simplified system diagram

Diagram shows a closed, reversible system that consists of metal hydride system and BPAM system. The actuation is initiated by change of temperature metal hydride element. In which, desorbs or absorbs H₂ gas that results in contraction or expansion of muscle. Thermoelectric device heats the metal hydride to raise temperature. Here, electrical energy is converted into heat where it results in the release of H₂ gas. As the device heats up and more hydrogen is released, the gas pressurizes BPAM [2]. Then, BPAM contracts fully after being pressurized. The contraction results in negative displacement change. Hence, the displacement change in BPAM creates a pulling force. Whereas, cooling process produces an effect that is vice versa [10]. By the way, a clearer picture of the process can be viewed in the following diagram, Figure 2.7.

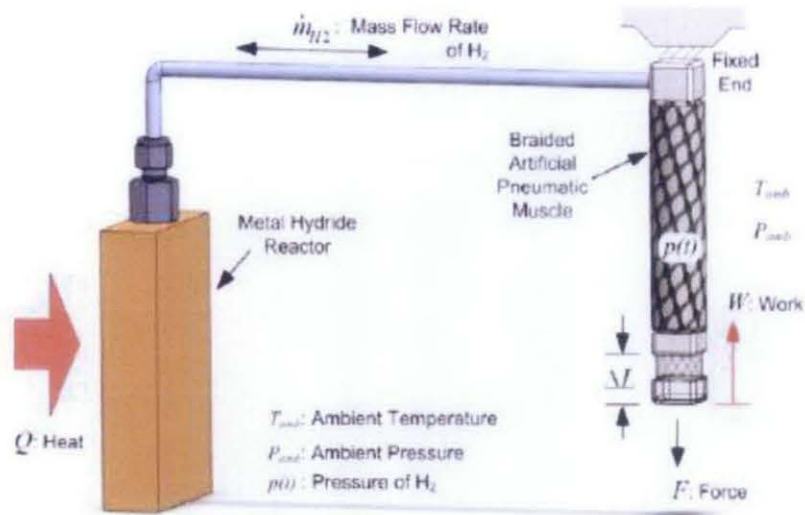


Figure 2.7: Schematic diagram of a metal hydride driven braided artificial pneumatic muscle (BPAM) [10].

Coupled BPAM-metal hydride system has an advantage by being compact, lightweight, noiseless, and by having high force-to-weight ratio compared to other fluidic system/ storage. There are two possible designs of metal hydride system that can be implemented in this project. These designs will provide a rough idea on designing a metal hydride system in this project. Following are Figure 2.8 and Figure 2.9 - the stated designs.

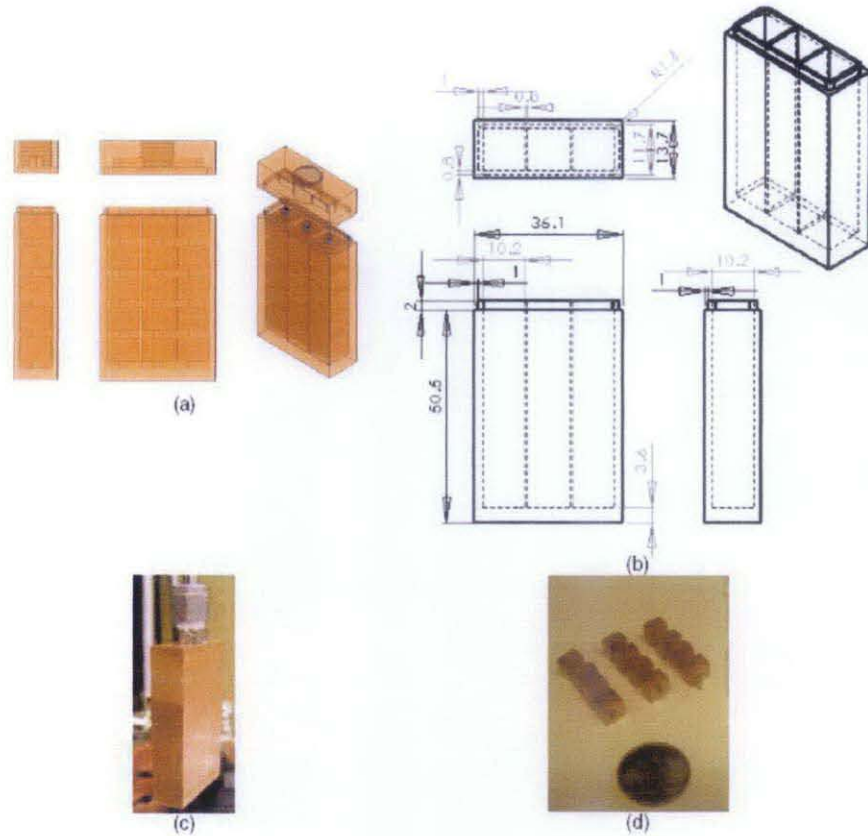


Figure 2.8: (a) and (b) Reactor containment unit design showing metal hydride pellets enclosed in reactor unit chambers, (c) actual sealed containment unit, and (d) metal hydride pellets [10].

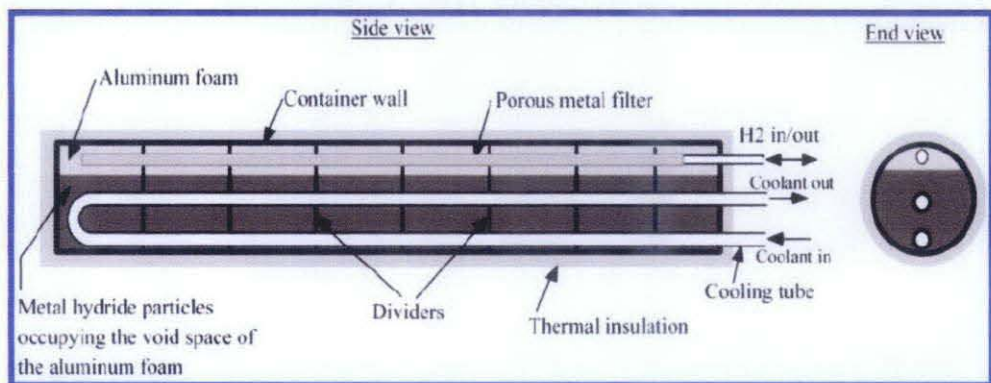


Figure 2.9: Schematic of the metal hydride hydrogen storage vessel [25]

2.4 Isentropic Processes [17- 22]

As mentioned above, the process involved in BPAM system is internally reversible and it is assumed to be adiabatic (no heat transfer for fully insulated metal hydride

system). It follows the principle of isentropic process, where the entropy remains constant.

It is characterized by the relation: $\Delta s = 0$ or $s_2 - s_1 = 0$

So, the H₂ gas will have the same entropy value at the end of the process as it does at the beginning. An isentropic process is an idealization of an actual process, and serves as a limiting case for an actual process. That means the actual process would not go more than the limit/ performance achieved from isentropic process. The equations below discuss the isentropic properties of gas. H₂ is assumed to show ideal gas behaviour throughout the experiment. Hence, it is feasible to follow the property relations of ideal gas.

Entropy Change of Ideal Gases

The property relations for ideal gases are:

$$Pv = RT$$

$$du = c_v dT$$

$$dh = c_p dT$$

$$Tds = du + Pdv$$

$$= c_v dT + RTdv/v$$

$$ds = c_v dT/T + Rdv/v$$

Integrating ds from state 1 to state 2 gives the first relation of entropy change for ideal gases.

$$\Delta s = s_2 - s_1 = \int_1^2 c_v \frac{dT}{T} + R \ln \frac{v_2}{v_1}$$

The relation of entropy change for ideal gases is obtained by replacing v by RT/P and dh by c_pdT. It is as follows:

$$Tds = dh - vdP$$

$$= c_p dT - RTdP/P$$

$$ds = c_p dT/T - R dP/P$$

Integrating ds from state 1 to state 2 gives the relation of entropy change for ideal gases as shown below:

$$\Delta s = s_2 - s_1 = \int_1^2 c_p \frac{dT}{T} - R \ln \frac{P_2}{P_1}$$

A common approximation is made by assuming that the specific heats of ideal gases are constants if the temperature variation is small (constant-specific-heats assumption). Replacing c_v and c_p with constants $c_{v,av}$ and $c_{p,av}$ in the first and second relations of entropy change and integrating from state 1 to state 2 gives,

$$\Delta s = s_2 - s_1 = c_{v,av} \ln \frac{T_2}{T_1} + R \ln \frac{v_2}{v_1} \quad \text{----- (1)}$$

$$\Delta s = s_2 - s_1 = c_{p,av} \ln \frac{T_2}{T_1} - R \ln \frac{P_2}{P_1} \quad \text{----- (2)}$$

By setting Δs to 0 in the above equations, the relations for an ideal gas which undergoes an isentropic process can be obtained. Simplified version of both equations is as listed:

$$c_v \ln \frac{T_2}{T_1} = -R \ln \frac{v_2}{v_1}$$

$$\frac{T_2}{T_1} = \left(\frac{v_2}{v_1} \right)^{R/c_v} = \left(\frac{v_2}{v_1} \right)^{k-1} \quad \text{----- (3)}$$

$$c_p \ln \frac{T_2}{T_1} = R \ln \frac{P_2}{P_1}$$

$$\frac{T_2}{T_1} = \left(\frac{P_2}{P_1} \right)^{R/c_p} = \left(\frac{P_2}{P_1} \right)^{\frac{k-1}{k}} \quad \text{----- (4)}$$

$$\left(\frac{P_2}{P_1} \right)^{\frac{k-1}{k}} = \left(\frac{v_1}{v_2} \right)^k \quad \text{----- (5)}$$

where

$$k = \text{specific heat ratio, } k = c_p/c_v \text{ and } R = c_p - c_v$$

2.5 Ideal Gas Law

The hydrogen gas desorption by metal hydride in this context is classified as ideal gas. Hydrogen gas obeys the ideal gas law at low pressure (< 10 bar) and low temperature with negligible deviation. Ideal gases are defined as:

- a) The volume of gas molecules is insignificant compared with the total volume enclosing the gas.
- b) No attractive or repulsive forces exist among the molecules or between the molecules and the container walls.
- c) All molecule collisions are perfectly elastic; i.e., there is no loss of internal energy upon collision

An equation describing the relationship between the volume occupied by a gas, the pressure and the temperature is called equation of states. It was observed that Boyle's Law and Charles Law constitute the equation of states for an ideal gas, that is:

$$PV = nR_u T \quad \text{----- (6)}$$

$$PV = mRT \quad \text{----- (7)}$$

Where,

P = pressure of the gas (kPa)

V = volume of the gas in (m³)

n = number of moles (mol)

R_u = universal gas constant (kPa. m³/ kmol. K)

T = temperature (K)

m = mass of gas (kg)

R = individual gas constant (kPa. m³/ kg. K)

2.6 Relationship Volumetric H₂ density vs Gravimetric H₂ Density

The most available and commonly used metal hydrides have been researched for its chemical and physical properties and also, its storage capacity. Storage capacity has been interpreted into a volumetric H₂ density vs gravimetric H₂ density graph to show types of hydrogen storage components and materials with their characteristic of storage capacity by mass and volume H₂ densities (in other words, stored hydrogen per mass and per volume is shown). Figure 2.10 interprets the overview of hydrogen storage properties.

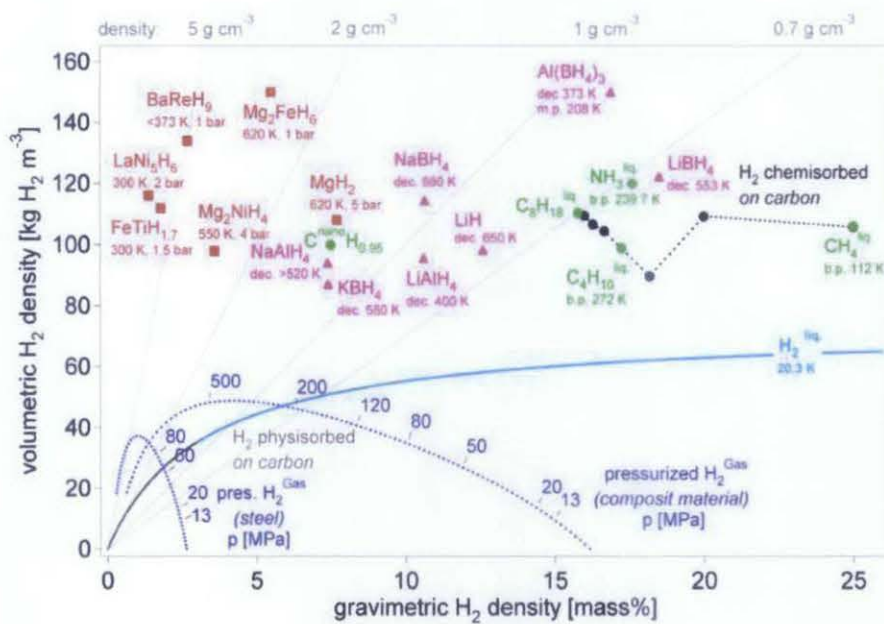


Figure 2.10: Relationship of stored hydrogen per mass and per volume in volumetric H₂ density vs gravimetric H₂ density graph. From A. Zuttel (2004). Hydrogen storage methods. *Naturwissenschaften* 91, 157-172. [15]

The lecturers from Delft University of Technology (in cooperation with Energy Research Centre of the Netherlands) have reviewed the diagram above to calculate hydrogen storage for mobile applications. Their result of calculation has been published in a presentation as in the Figure 2.11.

Hydrogen storage for mobile applications

Example:
Suppose 3 litre (2.4 kg) gasoline/100km.
This is equivalent with 0.8 kg hydrogen for 100 km.

For 500 km 4 kg of hydrogen is required.
This requires 300 kg of metal-hydride!
(LaNi_5H_6 1.4 wt.%)

$\Delta H = -35 \text{ kJ/mol H}_2$
4 kg hydrogen fuelling in 160 sec results in 434 kW heat to be dissipated



Ref.: Louis Schlapbach & Andreas Züttel, NATURE | VOL 414 | 15 NOVEMBER 2001 | pp. 353-358

46

Energy research Centre of the Netherlands

www.ecn.nl

Figure 2.11: The calculated volume and weight of hydrogen storage for mobile application [15]

The calculated results are based on the graph shown in Figure 2.10. They have referred to the storage properties with respect to volumetric H_2 density and gravimetric H_2 density. Take LaNi_5H_6 for example. They have proven that for 500km, 4kg of hydrogen is required. Hence, their calculation resulted in need of 300kg of LaNi_5H_6 , which was calculated based on the gravimetric H_2 density (1.4 wt.%), whereas the volume – 33 litres is defined through the analysis of proportionality theorem of volumetric H_2 density analysis.

Sample calculation:

From the graph, LaNi_5H_6 at 300K, 2 bar has storage capacity with: -

$$\text{Volumetric H}_2 \text{ density} = 120 \text{ kg H}_2 \text{ m}^{-3}$$

$$\text{Gravimetric H}_2 \text{ density} = 1.4 \text{ wt.}\%$$

With this,

$$V = 4\text{kg H}_2 / 120 \text{ kg H}_2 \text{ m}^{-3}$$

$$= 33\text{L of LaNi}_5\text{H}_6$$

$$m = (4\text{kg} / 1.3 \text{ wt}\%) \times 100$$

$$= 300\text{kg of LaNi}_5\text{H}_6$$

2.7 Natural Limb Structure & Artificial Limb Structure

There are similarities between the artificial muscle and human arm behaviour. The action of BPAM is analogous to the behaviour of biceps or triceps muscle in human arm. The first invention to mimic the behaviour of natural muscle was McKibben muscle which was invented in 1950s with the aim of helping poliomyelitic patients as a substitute for their weak muscular structure. However for this project, BPAM is favourably used as it is proved by journals to be very reliable.

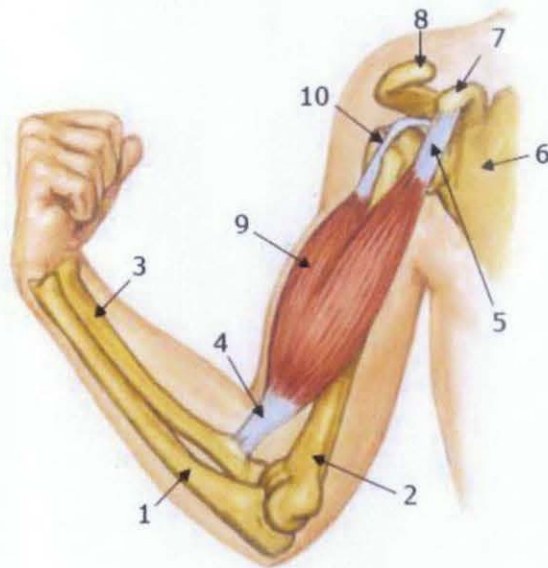


Figure 2.12: The biceps muscle in human arm

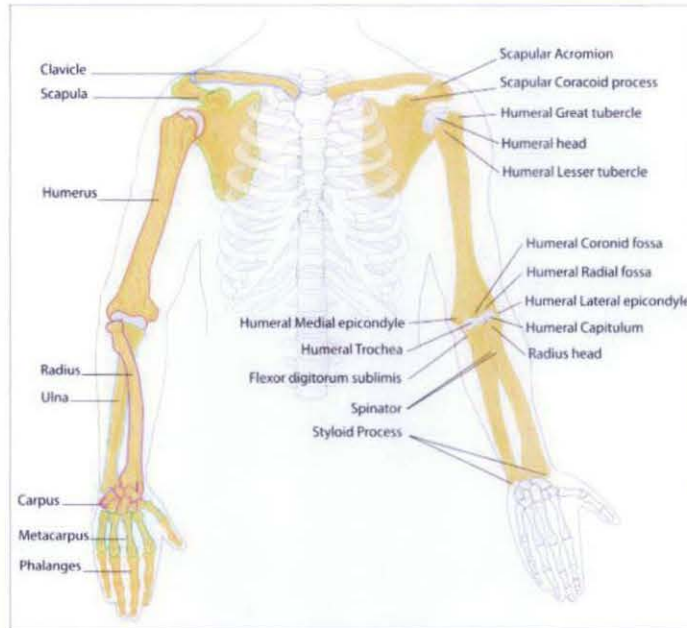


Figure 2.13: The bone structure in upper limbs

The Biceps is attached to the forearm bone called the radius and originates at the scapula in two places. The Biceps runs down the anterior or front side of the humerus and makes up approximately 1/3 of the muscle mass of the upper arm. The parts of structure shown in Figure 2.12 are:

1. Ulna
2. Humerus
3. Radius
4. Biceps tendon
5. Short head of biceps tendon
6. Scapula
7. Coracoid process
8. Acromion process
9. Biceps
10. Long head of biceps tendon

This information can be used to design the artificial limb needed for this project. It will very well aid the design of artificial limb to be used for the people who need it and as a prototype for BPAM-load system.

CHAPTER 3

METHODOLOGY

3.1 Flow of Tasks

Metal hydride system

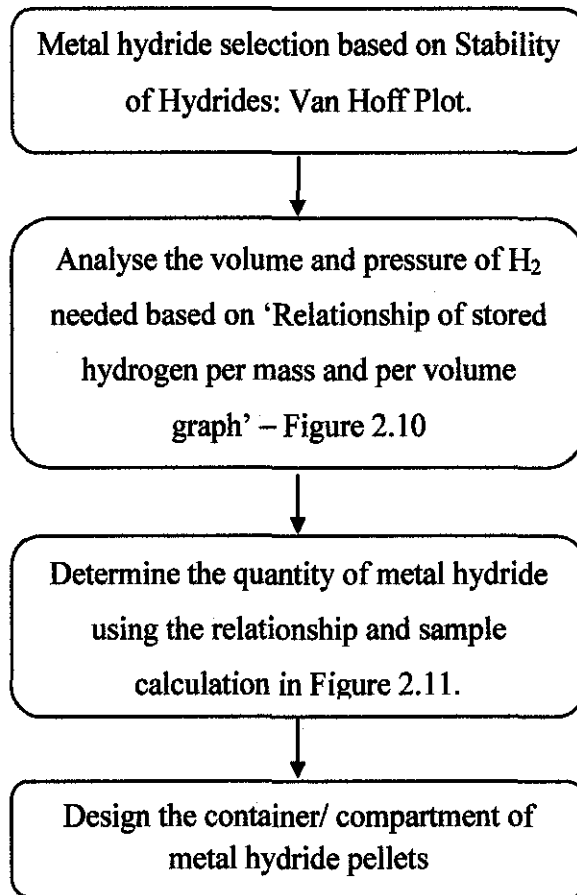


Figure 3.1: Task flow for metal hydride system

BPAM system (Artificial Arm & Artificial Muscle)

1. Study human arm structure and measure its components for sketching.
2. Sketch with proper dimensions and draft with Catia 3D.
3. Simulation with ANSYS for its expansion and contraction:-

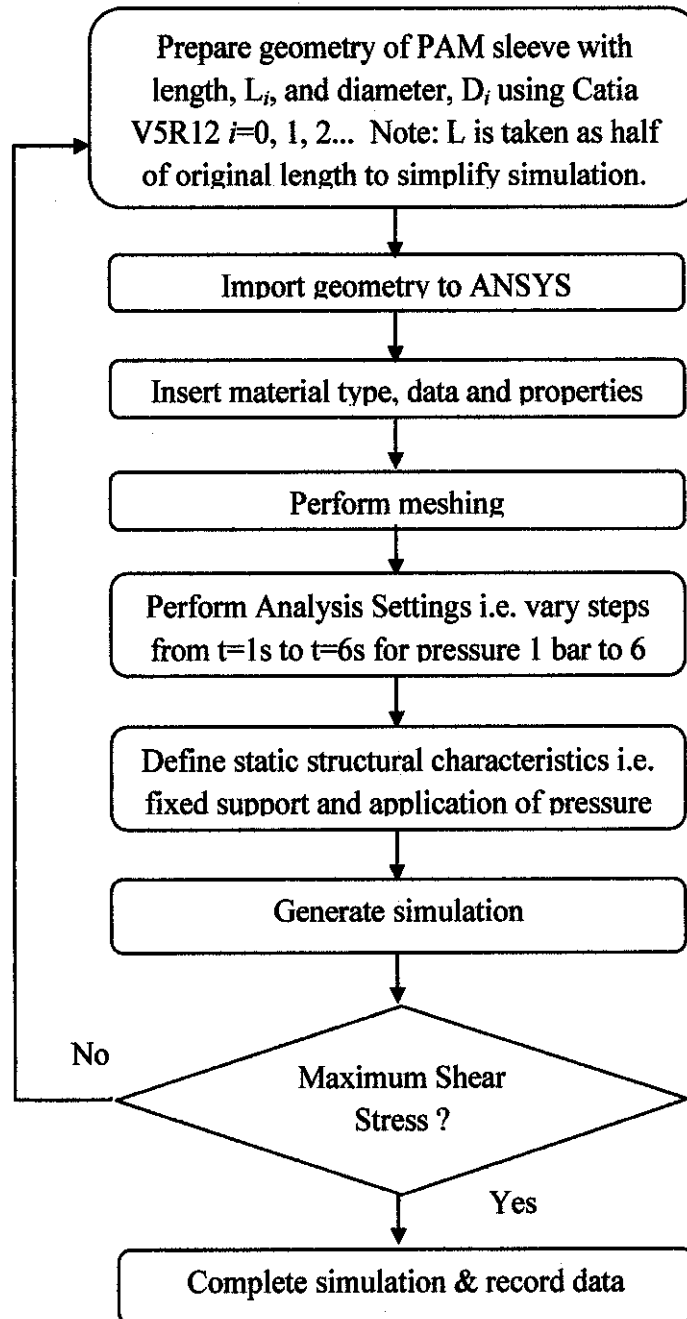


Figure 3.2: Task flow for PAM simulation i.e. radial expansion and axial contraction

3.2 Project Planning, Work Done & Gantt Chart

	Week (Semester 1)													
Tasks	1	2	3	4	5	6	7	8	9	10	11	12	13	14
Title confirmation and gather project information	■	■												
Material selection of metal hydride.			■	■										
Analyse the volume and pressure of H ₂ needed.					■									
Design the container of metal hydride						■	■	■						
Determine the quantity of metal hydride									■	■				
Design of BPAM-load system.											■	■	■	■

	Week (Semester 2)													
Tasks	1	2	3	4	5	6	7	8	9	10	11	12	13	14
Simulation with ANSYS for its expansion and contraction	■	■	■	■	■	■	■	■	■	■	■	■	■	■
Results & Discussion												■	■	■

Legend: -

■ : Shows the work done

Table 3.1: Gantt chart of Semester 1 & 2

CHAPTER 4

INITIAL RESULTS & DISCUSSION

4.1 Material Selection

Throughout the four weeks, extensive journals were read to provide insight to this project. The insight has given relevant knowledge, and concepts about the project. The figure below was the guide for metal hydride selection. The diagram, Figure 4.1 shows the stability of hydrides at given temperature ($^{\circ}\text{C}$) and pressure (MPa) for stated metal hydride.

For this project, the preferred operating temperature is above 25°C and max operating pressure is 600kPa. It should be observed that at 25°C , the hydride must be able to produce 1atm of pressure so that, the BPAM is at 'rest' at room temperature. Thus, the boundary limits set as criterion for selection are:

- a) 25°C and 1atm is marked with light blue
- b) maximum pressure that is required (600kPa or 6 bars) for BPAM is marked with red dashed line

By setting room temperature as lowest temperature limit that is around 25°C , the only hydride which behaves almost idle is NaAlH_4 – having 100kPa of pressure at 1 atm. The region of the material is marked with orange ellipse. Sodium aluminium hydride can release up to 600kPa of H_2 gas at 75°C . This comparatively low operating temperature is suitable for the actuation system [15]. It is stable within that temperature.

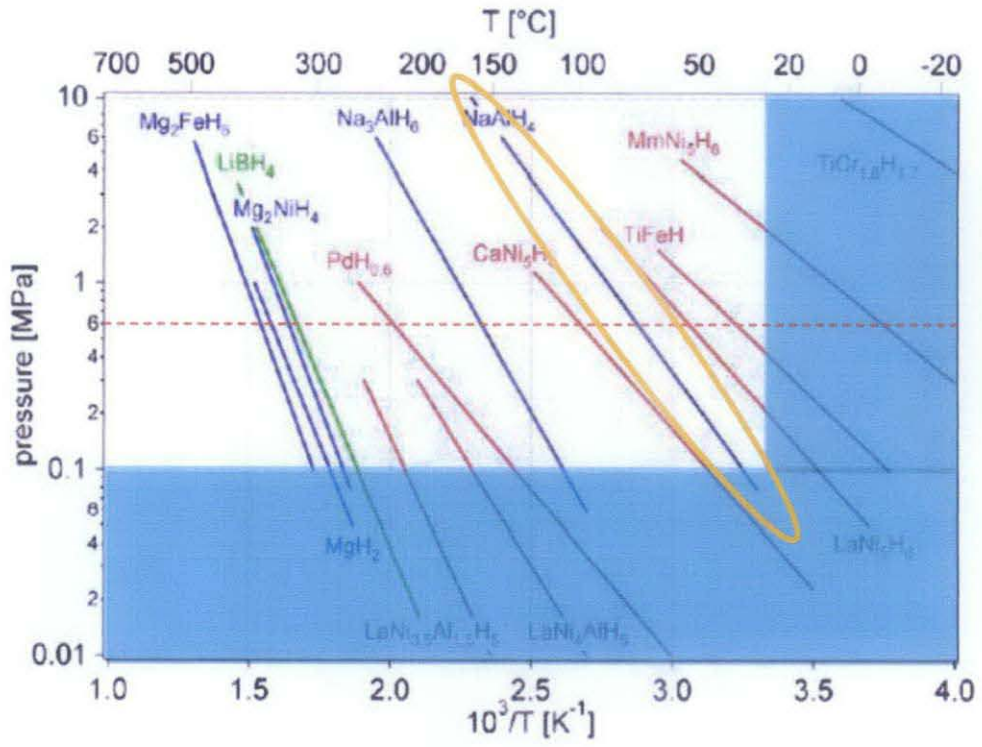


Figure 4.1: Stability of Hydrides: Van't Hoff Plot [15]

4.2 Analyses of volume and pressure of H₂ needed for 3 varied diameters

The analysis of H₂ gas volume needed is done by constraining the pressure that can be applied to BPAM. The maximum Pressure that BPAM can withstand is = 6 bar and the ambient pressure is set to be 1 bar [24]. Hence using this limitation, the isentropic volume change is calculated using the formulas that have been listed above in Literature Review. Three different diameters of BPAM samples have been analysed; with D₁=10mm, D₂= 20mm, D₃=30mm.

Table 4.1: Isentropic process analyses with Pressure change from 1 to 6 bars

D (m)	L (m)	V _{1(PAM)} (m ³)	V _{2(PAM)} (m ³)	V _{2 (gas)} (m ³)	V _{1(gas)} (m ³)
1.00E-02	1.40E-01	1.10E-05	1.37E-05	1.37E-05	1.99E-05
2.00E-02	1.40E-01	4.40E-05	5.50E-05	5.50E-05	7.94E-05
3.00E-02	1.40E-01	9.90E-05	1.24E-04	1.24E-04	1.79E-04

First of all, it is assumed that maximum possible expansion for BPAM is 25% [24]. Using the information, maximum expanded volume is calculated and shown for each of the BPAM sample. The table above analyses isentropic process with pressure change without considering temperature change in 3 BPAM samples. V₂ of BPAM was set as the final volume for H₂ gas since, gas experiences compression under high pressure. Thus, the final volume after the compression will be the desired expanded volume of BPAM. From the table, the highest volume of gas that is required is 1.79E-04m³. Although the temperature for this application could reach up to 75°C (350 K), the temperature range can be ignored because the gas lose heat to the environment via BPAM. The gas temperature will return to room temperature. So, only the temperature of hydride is maintained at 75°C, while the gas is not affected by the heating as it will cool to room temperature.

Finally, it can be concluded that to achieve full capacity in BPAM, maximum volume of H₂ required is 1.79E-04m³. So, this volume will be used to find the needed metal hydride quantity.

4.3 Required Mass of Sodium Aluminium Hydride, NaAlH₄

To find the required mass of the metal hydride, first it is important to find the mass of hydrogen that will be used for the expansion of BPAM. The amount of hydrogen released will determine whether BPAM expands to the optimum length or else. By referring to previous information, the maximum pressure is set to be= 6 bar, the ambient pressure is set to be 1 bar [24] with 298K temperature, and, the allowable maximum temperature is 350K. This information showed that required gas is 1.79E-04m³.Hence, the mass of H₂ is calculated using the Ideal Gas Law, where R= 4.124 kPa.m³/kg.K

$$PV = mRT$$

$$m = \frac{PV}{RT}$$

$$= \frac{(600)(1.79E-04)}{(4.124)(300)}$$

$$= 8.68E-05 \text{ kg}$$

Then, mass and volume of sodium aluminium hydride is calculated through the relativity of gravimetric and volumetric H₂ density. The metal hydride is marked with a black circle around it, as shown in the following diagram.

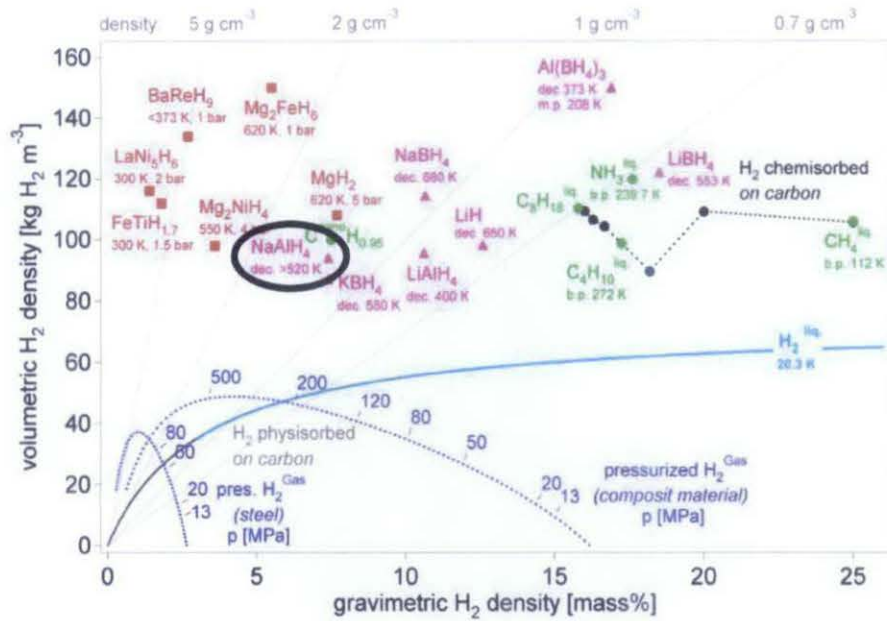


Figure 4.2: NaAlH₄ & its relationship of stored hydrogen per mass and per volume in volumetric H₂ density vs gravimetric H₂ density graph. [15]

Using the details from the relationship of stored hydrogen per mass and per volume diagram, it is known that:

Gravimetric density = 7.5 wt%

Volumetric density = 95 kg H₂.m⁻³

Thus, by performing calculation with the acquired data (as shown in Topic 2.1.5), the mass and volume required for the expansion of BPAM is displayed in the Table 3.

$$V = 8.68E-05 \text{ kg H}_2 / 95 \text{ kg H}_2 \text{ m}^{-3}$$

$$= 9.138E-07 \text{ m}^3$$

$$= \underline{0.914 \text{ cm}^3 \text{ of NaAlH}_4}$$

$$m = (8.68E-05 \text{ kg} / 7.5 \text{ wt}\%) \times 100$$

$$= 1.157E-03 \text{ kg}$$

$$= \underline{1.157\text{g of NaAlH}_4}$$

Table 4.2: Mass & Volume of Hydride Required

Mass (g)	~1.2
Volume (cm ³)	0.914

According to the calculated volume, it is desirable to design a container that is large enough to accommodate the hydride pellets for the ease of handling the material. The possible size of cubic shaped container for 0.914cm^3 hydride would be $2\text{cm} \times 2\text{cm} \times 2\text{cm}$, where it would be able to accommodate 2 pellets of hydride or 1.828cm^3 . 2 pellets are used to provide adequate gas in case of dysfunctional hydride pellets and also facilitate faster hydrogen gas absorption and desorption.

4.4 Artificial Arm (BPAM-Load System)

In analogous to natural human arm structure, mobility and behaviour, the artificial arm has been created. It looks almost identical to the natural arm with similar arm motion. The whole arm contains all the main parts of a natural arm, such as:

- Shoulder (scapula)
- Upper arm (humerus)
- Lower arm (radius and ulna)
- Wrist
- Joints
- Hands with fingers (acts as a structure to carry or hold a load)

The following diagrams are made as light as possible by removing excess material to make it hollow. It should be noted that, artificial shoulder can be joined together with the body of a patient. It is due to the extra length of the structure that makes it possible to be joined. Other than that, the hand with finger has a pocket where load can be placed on it.

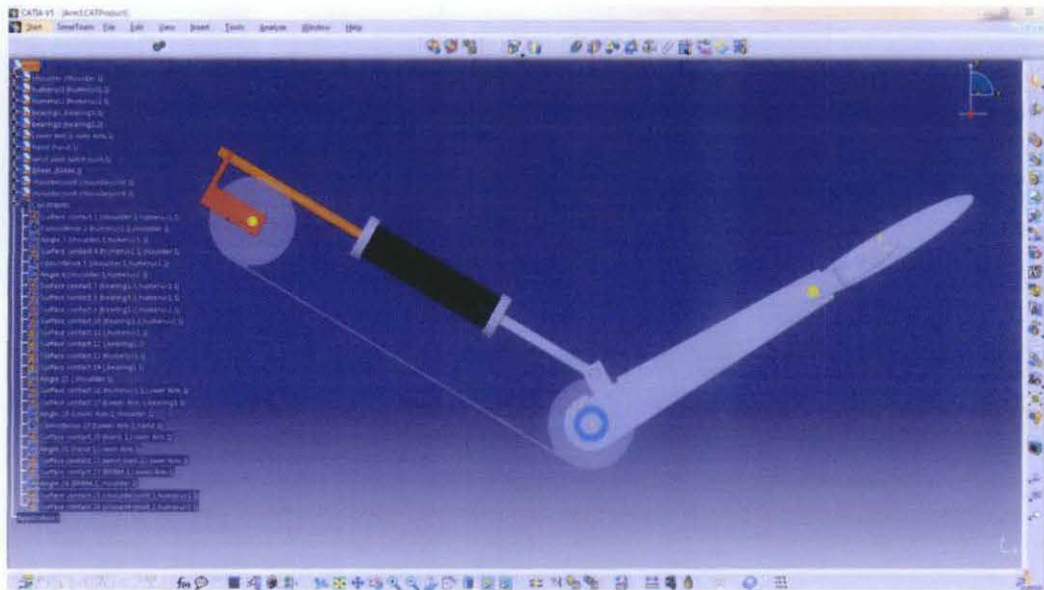


Figure 4.3: Artificial arm

The prototype design of artificial arm is such that:-

- a) The shoulder (red) is designed to be tied to upper body (scapula)
- b) The pipe (orange) is the hydrogen gas pipe-way that is to be connected to hydride container
- c) BPAM (black) is connected to lower arm where it can lift the lower arm as shown
- d) The upper arm is to be very light and hollow to reduce weight
- e) Lower arm is made to be hollow to reduce weight as well
- f) The bearings (blue) are installed for smooth motion

Besides that, the metal hydride container that is the main component of pneumatic actuation is also designed separately. It would be connected to the BPAM through valves, barometer and leak free pipe. Thickness of it is made to be 7mm to withstand pressure.

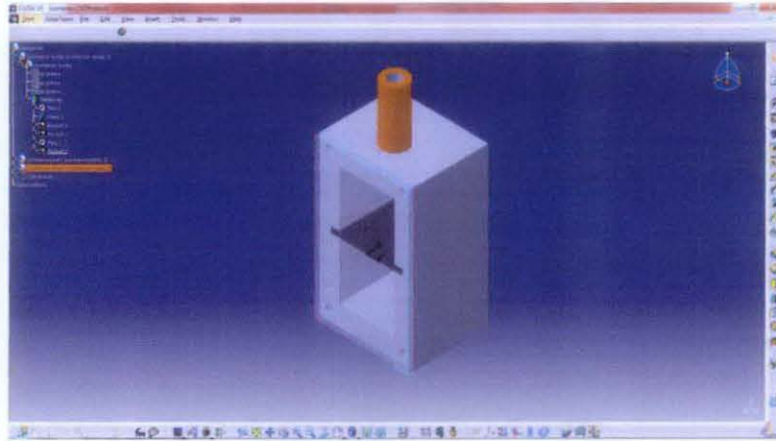


Figure 4.4: Hydride container

4.5 Simulation of BPAM

4.5.1 Simulation for $D=30\text{mm}$

The simulation is intended to approximate the percentage of contraction that a braided nylon sleeve can produce at 6 bars of pressure. The simulation in ANSYS has to be done in several iterations to achieve desired result due to:

- a) Silicone's elastic deformation effect on the sleeve
- b) Nylon sleeve behaviour which does not act like tube as specified by ANSYS

Hence, it prompted to do multiple iteration and simulation as had been indicated in Methodology. The results from ANSYS for iterations, $i=1$ to $i=26$ are shown in screenshots. However for simplification, samples from $i=1$ and $i=2$ is explained in detail as follows.



Figure 4.5: Geometry for L_1, D_1

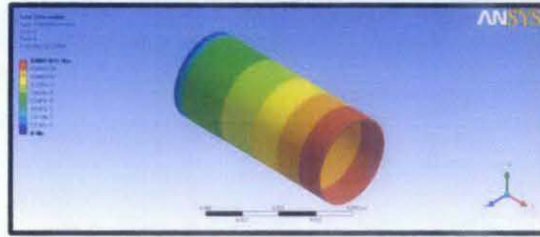


Figure 4.6: Total deformation for L_1, D_1

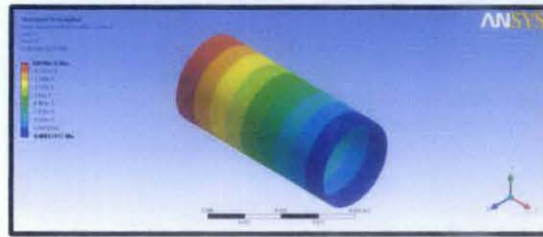


Figure 4.7: Directional deformation along X axis

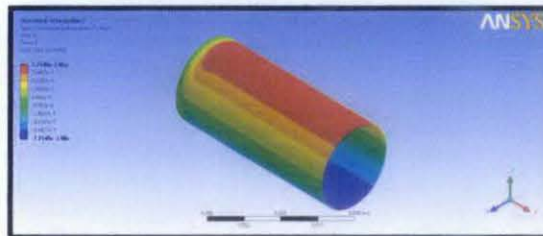


Figure 4.8: Directional Deformation along Y axis

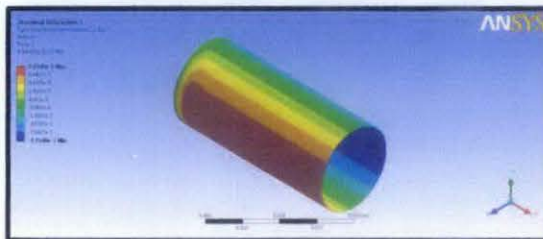


Figure 4.9: Direction Deformation along Z axis

L_1, D_1 is the original geometry that is imported from Catia to ANSYS. Figure 4.6, shows the total deformation experienced by the nylon sleeve. Figure 4.7, shows the deformation that occurs only at X axis. This result is used to calculate the percentage of contraction and the new length, L_2 . Directional deformation along Y and Z axis is approximately equal. Both define the maximum radial expansion. So, the new diameter, D_2 is known from here. A sample calculation below gives more detail on directional deformation.

In Figure 4.7, along the X axis, the original length, L_1 experiences contraction to L_2 .

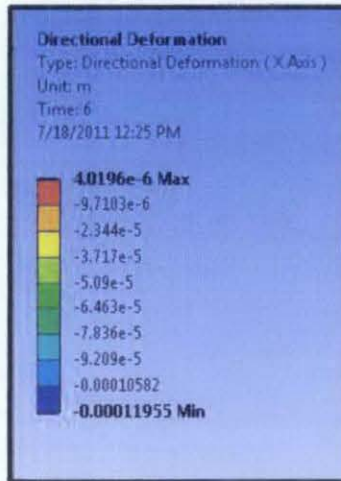


Figure 4.10: Values of bands along X axis

Total contraction is the sum of each colour bands in Figure 4.10. Each colour bands shows the value in displacement with unit, m. Hence,

$$L_2 = L_1 + (4.0196e-6 - 9.7103e-6 - 2.344e-5 - 3.717e-5 - 5.09e-5 - 6.463e-5 - 7.836e-5 - 9.209e-5 - 0.00010582 - 0.00011955)$$

$$L_2 = (70e-3) + (4.0196e-6 - 9.7103e-6 - 2.344e-5 - 3.717e-5 - 5.09e-5 - 6.463e-5 - 7.836e-5 - 9.209e-5 - 0.00010582 - 0.00011955)$$

$$L_2 = 69.422349\text{mm}$$

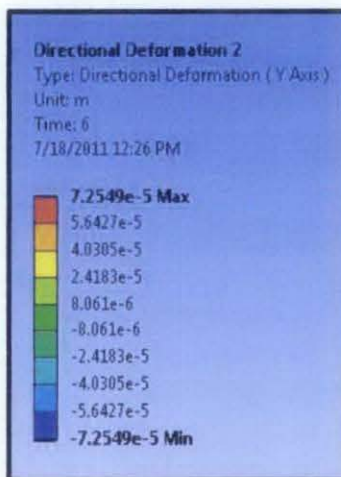


Figure 4.11: Values of bands along Y axis

Figure 4.8 shows the deformation along Y axis from $D_1/2$ to $D_2/2$. On the other hand, Figure 4.11 shows the values of deformation. Since, the deformation is only in radial length, the maximum deformation experienced by the nylon sleeve is recorded. Maximum deformation = $7.2549e-5m$ at Y and also Z axis. Hence,

Total deformation = Directional deformation at Y + Directional deformation at X

$$\text{Total deformation} = 7.2549e-5m + 7.2549e-5m = 2(7.2549e-5m)$$

So,

$$D_2 = D_1 + 2(7.2549e-5m) = 31mm + 0.145098mm = 31.145098mm$$

These results are recorded and used for second iteration, $i=2$. A new geometry is drawn in Catia for second iteration. Then, it is imported using ANSYS for simulation to find axial contraction and radial expansion. Axial contraction and radial expansion values are calculated and recorded for next iteration, $i=3$. This cycle of procedure is repeated until it reaches approximately maximum shear stress as shown in methodology. All iterations are recorded in table to display it in a graphical representation.

Table 4.3: Simulation and iteration results for L_i , D_i and percentage of contraction.

L_i	Length	Deform X	R	D	Deform Y	Contraction %
L_0	70.000000	0	15.500000	31.000000	0	0.00%
L_1	70.000000	0.5776507	15.500000	31.000000	0.072549	0.83%
L_2	69.422349	0.2633918	15.572549	31.145098	0.034764	1.20%
L_3	69.158958	0.3007425	15.607313	31.214626	0.035626	1.63%
L_4	68.858215	0.2646457	15.642939	31.285878	0.035934	2.01%
L_5	68.593569	0.2984487	15.678873	31.357746	0.036117	2.44%
L_6	68.295121	0.2635811	15.714990	31.429980	0.036299	2.81%
L_7	68.031540	0.2970503	15.751289	31.502578	0.036471	3.24%
L_8	67.734489	0.2624871	15.787760	31.575520	0.036631	3.61%
L_9	67.472002	0.2620128	15.824391	31.648782	0.036803	3.99%
L_{10}	67.209989	0.2615399	15.861194	31.722388	0.036976	4.36%
L_{11}	66.948449	0.2610635	15.898170	31.796340	0.037147	4.73%
L_{12}	66.687386	0.2605858	15.935317	31.870634	0.037321	5.10%
L_{13}	66.426800	0.2601123	15.972638	31.945276	0.037495	5.48%
L_{14}	66.166688	0.2596370	16.010133	32.020266	0.037668	5.85%
L_{15}	65.907051	0.2591659	16.047801	32.095602	0.037853	6.22%
L_{16}	65.647885	0.2588024	16.085654	32.171308	0.038032	6.59%
L_{17}	65.389083	0.2582350	16.123686	32.247372	0.038184	6.96%
L_{18}	65.130848	0.2254509	16.161870	32.323740	0.038205	7.28%
L_{19}	64.905397	0.2577568	16.200075	32.400150	0.038378	7.65%
L_{20}	64.647640	0.2572775	16.238453	32.476906	0.038550	8.01%
L_{21}	64.390362	0.2568066	16.277003	32.554006	0.038726	8.38%
L_{22}	64.133556	0.2559507	16.315729	32.631458	0.039108	8.75%
L_{23}	63.877605	0.2554659	16.354837	32.709674	0.039297	9.11%
L_{24}	63.622139	0.2549832	16.394134	32.788268	0.039457	9.48%
L_{25}	63.367156	0.2545077	16.433591	32.867182	0.039633	9.84%
L_{26}	63.112648	0.2537656	16.473224	32.946448	0.039802	10.20%
L_{27}	62.858883	0.0000000	16.513026	33.026052	0.000000	10.20%

After 26 iterations, the nylon sleeve started to deform abnormally. Due to this, the simulation is stopped at $i=26$ with such results. Thus, the final iteration results are $L_{27}= 62.858883\text{mm}$ and $D_{27}= 33.026052\text{mm}$ with 10.20% of contraction. Next diagram portrays graphical deformation at its full length.

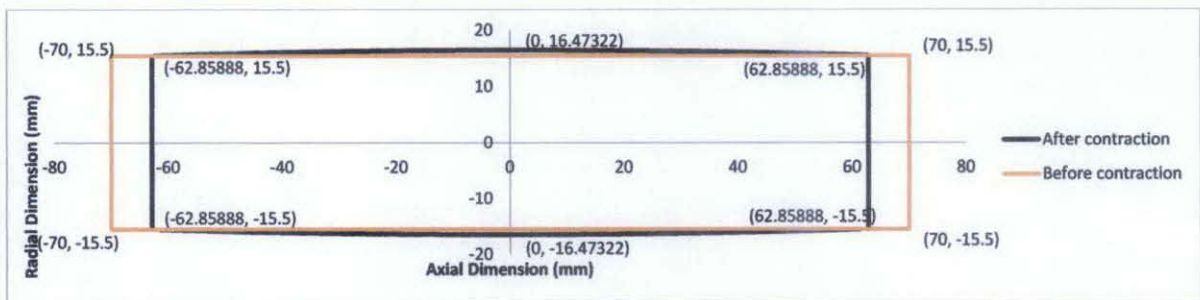


Figure 4.12: Graphical representation of the iteration results

The representation above shows maximum contraction at its axial length and expansion at its radial length. Axially, it has contracted from 140mm to 125.71mm, where the stroke is 14.28mm. Whereas radially, it had expanded from $R=15.5\text{mm}$ to $R=16.47\text{mm}$, 6.54%. The shape of deformation depicts silicon's elastic behaviour. For comparison, journal [3] has been referred. Figure that follows shows their results.

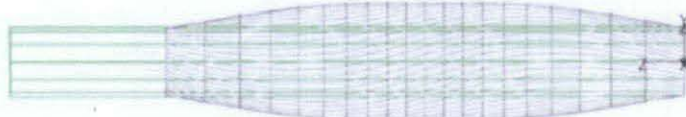


Figure 4.13: Linear static FEA results

Clearly, the shape of deformation is identical. The difference here is the software that is used for Finite Element Analysis.

4.5.2 Simulation for D=20mm

Similar to the procedure above, simulation and iteration has been done until there is abnormally high stress and deformation.

Table 4.4: Simulation and iteration results for L_i , D_i and percentage of contraction.

L_i	Length	Deform X	R_i	D_i	Deform Y	Contraction %
L ₀	70.000000	0	10.500000	21.000000	0	0.00%
L ₁	70.000000	0.3874695	10.500000	21.000000	0.032854	0.55%
L ₂	69.612531	0.1745406	10.532854	21.065708	0.015544	0.80%
L ₃	69.437990	0.1743479	10.548398	21.096796	0.015539	1.05%
L ₄	69.263642	0.1741384	10.563937	21.127874	0.015683	1.30%
L ₅	69.089504	0.1769159	10.579620	21.159240	0.015707	1.55%
L ₆	68.912588	0.1739698	10.595327	21.190654	0.015759	1.80%
L ₇	68.738618	0.1737918	10.611086	21.222172	0.015813	2.05%
L ₈	68.564826	0.1736117	10.626899	21.253798	0.015867	2.30%
L ₉	68.391214	0.1734287	10.642766	21.285532	0.015921	2.55%
L ₁₀	68.217786	0.1730887	10.658687	21.317374	0.015950	2.79%
L ₁₁	68.044697	0.1728514	10.674637	21.349274	0.016030	3.04%
L ₁₂	67.871846	0.1727809	10.690667	21.381334	0.016203	3.29%
L ₁₃	67.699065	0.1725153	10.706870	21.413740	0.016191	3.53%
L ₁₄	67.526549	0.1722929	10.723061	21.446122	0.016142	3.78%
L ₁₅	67.354257	0.1721406	10.739203	21.478406	0.016298	4.03%
L ₁₆	67.182116	0.1719807	10.755501	21.511002	0.016378	4.27%
L ₁₇	67.010135	0.1717787	10.771879	21.543758	0.016408	4.52%
L ₁₈	66.838357	0.1716746	10.788287	21.576574	0.016529	4.76%
L ₁₉	66.666682	0.1714246	10.804816	21.609632	0.016505	5.01%
L ₂₀	66.495257	0.1712196	10.821321	21.642642	0.016572	5.25%
L ₂₁	66.324038	0.1710442	10.837893	21.675786	0.016629	5.50%
L ₂₂	66.152994	0.1708668	10.854522	21.709044	0.016686	5.74%
L ₂₃	65.982127	0.1707103	10.871208	21.742416	0.016736	5.98%
L ₂₄	65.811416	0.1704987	10.887944	21.775888	0.016819	6.23%
L ₂₅	65.640918	0.1703107	10.904763	21.809526	0.016838	6.47%
L ₂₆	65.470607	0.1701350	10.921601	21.843202	0.016933	6.71%
L ₂₇	65.300472	0.1699341	10.938534	21.877068	0.016940	6.96%
L ₂₈	65.130538	0.1697925	10.955474	21.910948	0.017091	7.20%
L ₂₉	64.960745	0.1695739	10.972565	21.945130	0.017078	7.44%

L ₃₀	64.791172	0.1694257	10.989643	21.979286	0.017204	7.68%
L ₃₁	64.621746	0.1692246	11.006847	22.013694	0.017168	7.92%
L ₃₂	64.452521	0.1690161	11.024015	22.048030	0.017270	8.17%
L ₃₃	64.283505	0.1688214	11.041285	22.082570	0.017303	8.41%
L ₃₄	64.114684	0.1687378	11.058588	22.117176	0.017369	8.65%
L ₃₅	63.945946	0.0000000	11.075957	22.151914	0.000000	8.65%

After 34 iterations, the final results are $L_{35}= 63.945946\text{mm}$ and $D_{35}= 22.151914\text{mm}$ with 8.65% of contraction. Next diagram portrays graphical deformation at its full length.

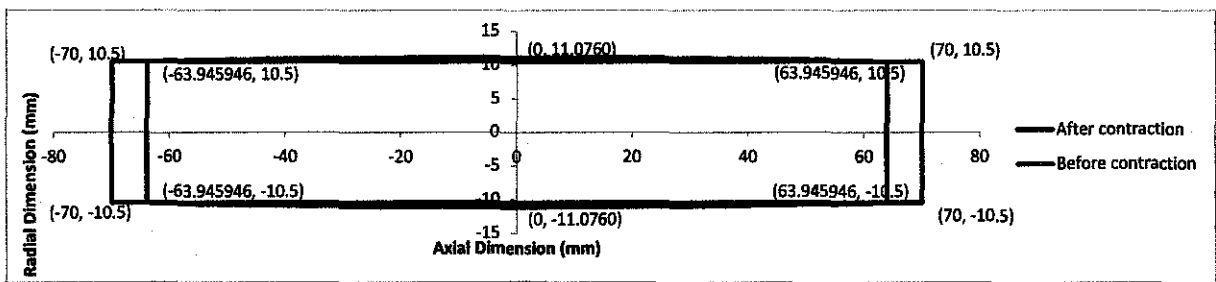


Figure 4.14: Graphical representation of the iteration results

The representation shows maximum contraction at its axial length and expansion at its radial length. Axially, it has contracted from 140mm to 127.89mm, where the stroke is 12.11mm. Whereas radially, it had expanded from R=10.5mm to R=11.08mm, 5.49%.

4.5.3 Simulation for D=10mm

Similar to the procedure above, simulation and iteration is done and shown below.

Table 4.5: Simulation and iteration results for L_i , D_i and percentage of contraction

L_i	Length	Deform X	R	D	Deform Y	Contraction %
L ₀	70.000000	0	5.500000	11.000000	0	0.00%
L ₁	70.000000	0.0804903	5.500000	11.000000	0.003685	0.11%
L ₂	69.919510	0.0804952	5.503685	11.007371	0.003692	0.23%
L ₃	69.839014	0.0804258	5.507377	11.014754	0.003695	0.34%
L ₄	69.758589	0.0804038	5.511072	11.022143	0.003926	0.46%
L ₅	69.678185	0.0803810	5.514997	11.029995	0.003933	0.57%
L ₆	69.597804	0.0803592	5.518930	11.037861	0.003940	0.69%
L ₇	69.517445	0.0804562	5.522870	11.045740	0.003852	0.80%
L ₈	69.436988	0.0804615	5.526722	11.053444	0.003858	0.92%
L ₉	69.356527	0.0804106	5.530580	11.061160	0.003863	1.03%
L ₁₀	69.276116	0.0810315	5.534443	11.068885	0.003920	1.15%
L ₁₁	69.195085	0.0816690	5.538362	11.076724	0.003978	1.27%
L ₁₂	69.113416	0.0821937	5.542340	11.084680	0.004141	1.38%
L ₁₃	69.031222	0.0828842	5.546482	11.092963	0.004213	1.50%
L ₁₄	68.948338	0.0835633	5.550694	11.101389	0.004109	1.62%
L ₁₅	68.864775	0.0841104	5.554803	11.109607	0.004522	1.74%
L ₁₆	68.780664	0.0802267	5.559325	11.118651	0.003900	1.86%
L ₁₇	68.700438	0.0802026	5.563225	11.126451	0.003906	1.97%
L ₁₈	68.620235	0.0801779	5.567131	11.134262	0.003911	2.09%
L ₁₉	68.540057	0.0801519	5.571042	11.142084	0.003916	2.20%
L ₂₀	68.459905	0.0799103	5.574958	11.149916	0.004112	2.31%
L ₂₁	68.379995	0.0799055	5.579070	11.158140	0.004141	2.43%
L ₂₂	68.300090	0.0798994	5.583211	11.166421	0.004039	2.54%
L ₂₃	68.220190	0.0799193	5.587249	11.174498	0.004044	2.66%
L ₂₄	68.140271	0.0469771	5.591293	11.182586	0.004049	2.72%
L ₂₅	68.093294	0.0798520	5.595342	11.190684	0.004056	2.84%
L ₂₆	68.013442	0.0797914	5.599398	11.198796	0.004175	2.95%
L ₂₇	67.933650	0.0638645	5.603573	11.207147	0.003264	3.04%
L ₂₈	67.869786	0.0798428	5.606838	11.213676	0.004068	3.16%
L ₂₉	67.789943	0.0797803	5.610906	11.221811	0.004078	3.27%
L ₃₀	67.710163	0.0797300	5.614983	11.229967	0.004187	3.39%
L ₃₁	67.630433	0.0797668	5.619171	11.238341	0.004088	3.50%

L ₃₂	67.550666	0.0796389	5.623259	11.246517	0.004185	3.61%
L ₃₃	67.471027	0.0796235	5.627444	11.254888	0.004223	3.73%
L ₃₄	67.391404	0.0796356	5.631667	11.263334	0.004218	3.84%
L ₃₅	67.311768	0.0796749	5.635884	11.271769	0.004119	3.95%
L ₃₆	67.232093	0.0795842	5.640003	11.280007	0.004232	4.07%
L ₃₇	67.152509	0.0795628	5.644235	11.288470	0.004235	4.18%
L ₃₈	67.072946	0.0794977	5.648470	11.296940	0.004239	4.30%
L ₃₉	66.993449	0.0801860	5.652709	11.305418	0.004243	4.41%
L ₄₀	66.913263	0.0795500	5.656952	11.313903	0.004120	4.52%
L ₄₁	66.833713	0.0794666	5.661071	11.322142	0.004259	4.64%
L ₄₂	66.754246	0.0794532	5.665331	11.330661	0.004282	4.75%
L ₄₃	66.674793	0.0795442	5.669613	11.339225	0.004093	4.86%
L ₄₄	66.595248	0.0794933	5.673706	11.347411	0.004162	4.98%
L ₄₅	66.515755	0.0793697	5.677867	11.355735	0.004284	5.09%
L ₄₆	66.436385	0.0793542	5.682151	11.364302	0.004313	5.20%
L ₄₇	66.357031	0.0793337	5.686464	11.372928	0.004208	5.32%
L ₄₈	66.277698	0.0792679	5.690672	11.381345	0.004342	5.43%
L ₄₉	66.198430	0.0792409	5.695014	11.390028	0.004286	5.54%
L ₅₀	66.119189	0.0793112	5.699300	11.398600	0.004206	5.66%
L ₅₁	66.039878	0.0792275	5.703506	11.407011	0.004322	5.77%
L ₅₂	65.960650	0.0791657	5.707828	11.415655	0.004276	5.88%
L ₅₃	65.881484	0.0792249	5.712104	11.424208	0.004223	6.00%
L ₅₄	65.802259	0.0790842	5.716327	11.432653	0.004412	6.11%
L ₅₅	65.723175	0.0791959	5.720738	11.441477	0.004245	6.22%
L ₅₆	65.643979	0.0791189	5.724983	11.449967	0.004279	6.34%
L ₅₇	65.564860	0.0791458	5.729262	11.458525	0.004194	6.45%
L ₅₈	65.485715	0.0791974	5.733456	11.466912	0.004293	6.56%
L ₅₉	65.406517	0.0790833	5.737749	11.475498	0.004311	6.68%
L ₆₀	65.327434	0.0790015	5.742060	11.484120	0.004275	6.79%
L ₆₁	65.248432	0.0790353	5.746335	11.492670	0.004272	6.90%
L ₆₂	65.169397	0.0789860	5.750607	11.501214	0.004250	7.01%
L ₆₃	65.090411	0.0789767	5.754857	11.509714	0.004341	7.13%
L ₆₄	65.011434	0.0788416	5.759198	11.518396	0.004468	7.24%
L ₆₅	64.932593	0.0788281	5.763666	11.527332	0.004478	7.35%
L ₆₆	64.853765	0.0788260	5.768144	11.536288	0.004412	7.46%
L ₆₇	64.774939	0.0787651	5.772556	11.545111	0.004522	7.58%
L ₆₈	64.696174	0.0000000	5.777078	11.554156	0.000000	7.58%

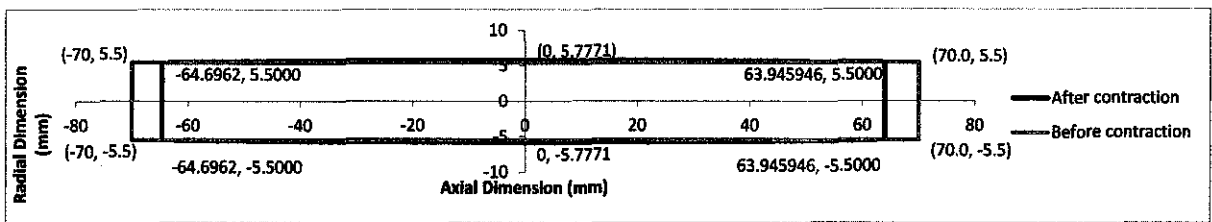


Figure 4.15: Graphical representation of the iteration results

The representation shows maximum contraction at its axial length and expansion at its radial length. After 68 iterations, the final results are $L_{68} = 64.696174$ and $D_{35} = 11.554$ mm with 7.58% of contraction i.e. from 140 mm to 129.39 mm with 10.61 mm stroke length. However, the radial expansion is not visible in this diagram. Radially it has expanded 0.277 mm, 5.03% of its diameter.

Comparisons between all three diameters are shown as follows. The results are comparative to journal [25] which shows result of 7% contraction in experiment for OD=30 mm.

Table 4.6: Difference between diameters

Diameter	Contraction (%)	Radial Expansion (%)
10	7.58	5.03
20	8.65	5.49
30	10.20	6.54

CHAPTER 5

CONCLUSION & RECOMMENDATIONS

5.1 Conclusion

Braided Pneumatic Artificial Muscle actuated by hydrogen gas is a good solution for upgrading existing robotic arm, industrial machines, and medical field. Sodium aluminium hydride has been chosen as the most suitable hydride for this application. The selected metal hydride - sodium aluminium hydride can release up to 600kPa of H_2 gas at $75^\circ C$. A very small amount of hydrogen gas, $1.79E-04m^3$ is stored in hydride to actuate BPAM when needed. In fact, the metal hydride makes this project to be classified as mobile structure because it only uses very small amount of sodium aluminium hydride, i.e. 1.2g with a volume of $0.914cm^3$. In addition, the metal hydride can provide a pressure of 6 bar to BPAM to contract 10.20% axially from 140mm to 125.71mm for $D=30mm$. Besides that, BPAM with $D=30mm$ contracts the most compared to 10mm, and 20mm. So, the artificial arm will be functional when BPAM is joined to the shoulder structure and lower arm structure which has been designed as prototype. However, more studies and experiments must be done to analyse maximum hoop stress, kinematics motion analysis to the arm, wall thickness of hydride container, and the reaction time of hydrogen gas absorption and desorption by hydride when heated and cooled.

5.2 Recommendations

Throughout the simulations and results, it provided an exposure to this project. However certain parameters have to be controlled, so that the practical prototype functions up to the desired expectations. Sound recommendations that can be done to create the best practical prototype are:

- a) To use very thin yet durable silicon tube for the containment of the gas. Thin tube deforms more as soon as pressure is applied. Hence, better percentage of contraction.
- b) To use frictionless material for the braided sleeve or wax may be used between strands to reduce friction and enhance smooth and complete 100 % expansion.

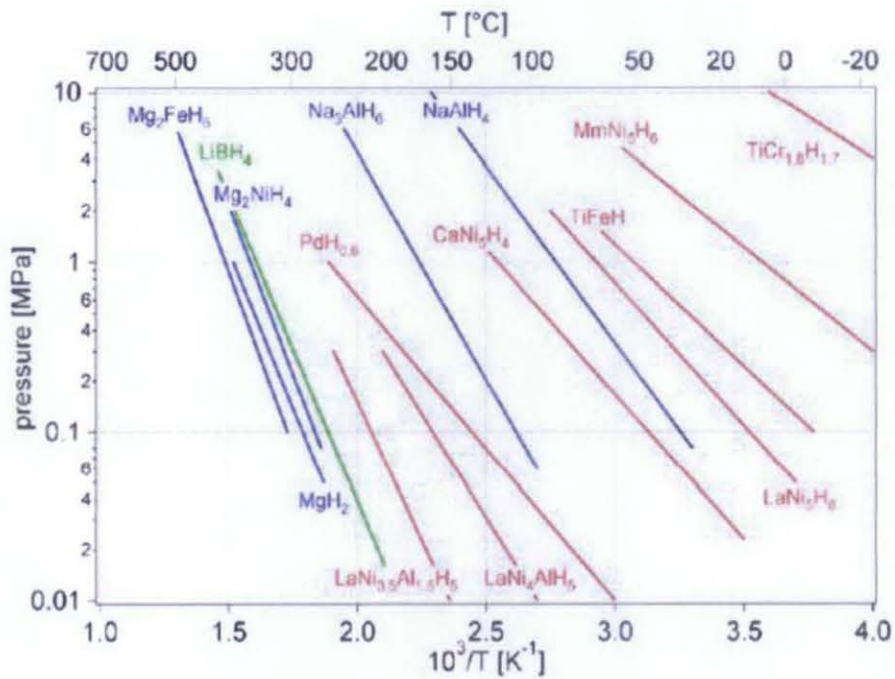
REFERENCES

- [1] Bertrand Tondu, and Pierre Lopez, 1997 The McKibben muscle and its use in actuating robot-arms showing similarities with human arm behaviour *Industrial Robot: An International Journal* ISSN: 0143-991X
- [2] Device Mimics Human Muscle Size, Strength; <http://news.discovery.com/tech/artificial-muscle-hydrogen-artificial.html>
- [3] R. Ramasamy, M.R. Juhari, M.R. Mamat, S.Yaacob, N.F Mohd Nasir, and M. Sugisaka; *An application of Finite Element to PAM*, 2005 *American Journal of Applied Science* 2 ISSN 1546-9239
- [4] B. Zhou, M. L. Accorsi and J. W. Leonard, 2004 *A new finite element for modeling pneumatic muscle actuators*
- [5] Christopher & Dana Reeve Foundation 2009 *One Degree of Separation: Paralysis and Spinal Cord Injury in the United States*
- [6] Zeljko Situm & Srecko Herceg; *Design & Control of Manipulator Arm Driven by PAM*, 2008 16th *Mediterranean Conf. on Control & Automation*
- [7] Kevin B. Fite, Thomas J. Withrow, Keith W. Wait, and Micheal Goldfarb; *A Gas Actuated Anthropomorphic Transhumeral Prosthesis*, *IEEE Int. Conf. on Robotics & Automation* April 2007.
- [8] D. B. Reynolds, D. W. Repperger, C. A. Phillips, and G. Bandry; *Modelling the Dynamic Characteristics of PAM*; *Annals of Biomedical Engineering*, Vol 31, pp310-317, 2003.
- [9] Frank Daerden, and Dirk Lefeber; *PAM: Actuators for Robotics & Automation*; *Vrije Universiteit Brussel, Department of Mechanical Engineering*.
- [10] Alexandra Vanderhoff, and Kwang J Kim; *Experimental Study of a Metal Hydride Driven BPAM*; *Smart Mater. Struct.* 18 (2009) 125015 (10pp).
- [11] Bottling the hydrogen genie; <http://www.aip.org/tip/INPHFA/vol-10/iss-1/p20.html>
- [12] Hydrogen Storage, Energy Resources Division; <http://www.bnl.gov/est/erd/hydrogenStorage/>
- [13] Solid State Hydrogen Energy; <http://www.ergenics.com/page14.htm>
- [15] A. Zuttel; *Hydrogen Storage Materials*; H2 Net Seminar, University of Birmingham, 16 December 2004.

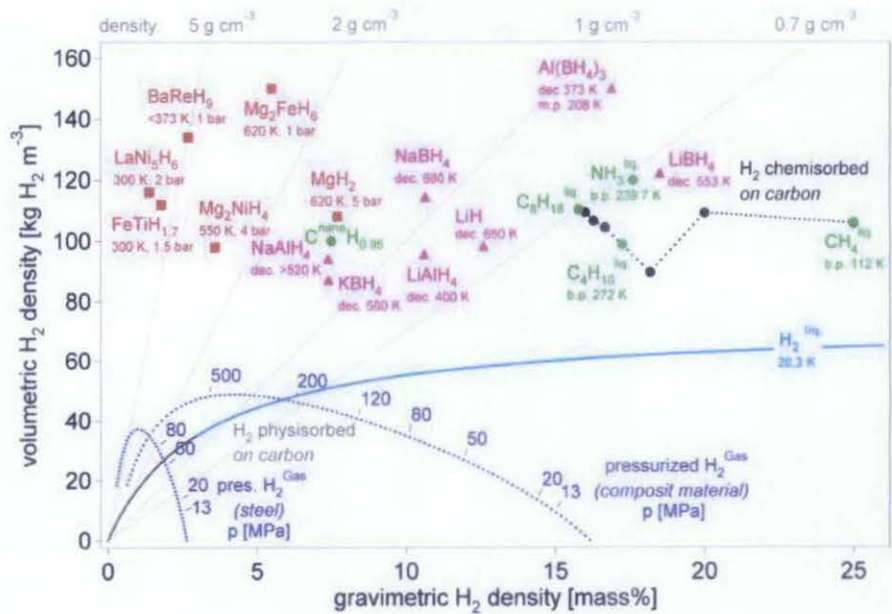
- [14] George M. Lloyd, Kwang J. Kim; *Smart hydrogen/ Metal Hydride Actuator, Int. Jour. Of Hydrogen Energy* 32 (2007) 247-255
- [16] F.S. Yang, G.X. Wang, Z.X. Zhang, X.Y. Meng and V. Rudolph; *Design of the metal hydride reactors – A review on the key technical issues*, International Journal of Hydrogen Energy.
- [17] Yunus A. Cengel, Micheal A. Boles; *Thermodynamics: An Engineering Approach, 6th edition*.
- [18] Jin-Kyeong Kim, Il-Seok Park, Kwang J. Kim, and Keith Gawlik; *A hydrogen-compression system using porous metal hydride pellets of $LaNi_{5-x}Al_x$* , International Journal of Hydrogen Energy Volume 33, Issue 2, January 2008, Pages 870-877.
- [19] Monterey R. Gardiner, Andrew Burke; *Comparision of Hydrogen Storage Technologies: A Focus on Energy Required For Hydrogen Input*, University of California.
- [20] NASA; *Isentropic Flow Equations*, <http://www.grc.nasa.gov/WWW/K-12/airplane/isentrop.html>
- [21] Thermodynamics E-book; *Isentropic Processes*, http://www.ecourses.ou.edu/cgi-bin/ebook.cgi?doc=&topic=th&chap_sec=06.4&page=theory
- [22] Thermodynamics E-book; *Entropy Change of Ideal Gas*, http://www.ecourses.ou.edu/cgi-bin/eBook.cgi?doc=&topic=th&chap_sec=06.3&page=theory
- [23] Festo; *Fluidic Muscle DMSP & Fluidic Muscles MAS*, [http://www3.festo.com/C1256D56002E7B89.nsf/html/info_501_en.pdf/\\$FILE/info_501_en.pdf](http://www3.festo.com/C1256D56002E7B89.nsf/html/info_501_en.pdf/$FILE/info_501_en.pdf)
- [24] S. Davis Darwin G. Caldwell; *Braid Effects on Contractile Range and Friction Modeling in Pneumatic Muscle Actuators*, University of Salford.
- [25] Sarang A. Gadre, Armin D. Ebner, Shaheen A. Al-Muhtaseb, and James A. Ritter; *Practical Modeling of Metal Hydride Hydrogen Storage Systems*, Ind. Eng. Chem. Res. 2003, 42, 1713-1722.
- [26] ??

APPENDIX A

1. Stability of Hydrides: Van't Hoff Plot [15]

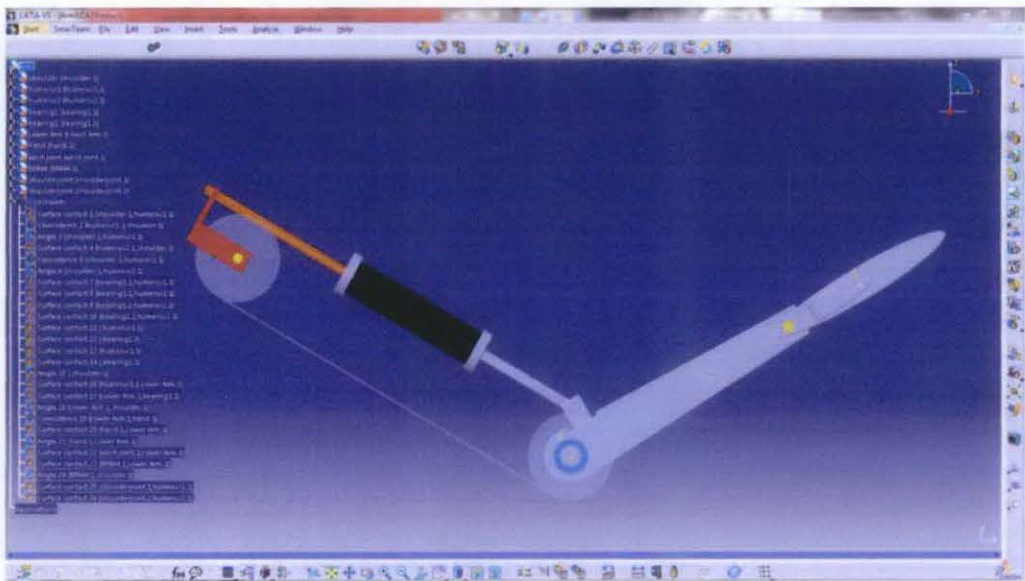


2. NaAlH₄ & its relationship of stored hydrogen per mass and per volume in volumetric H₂ density vs gravimetric H₂ density graph.

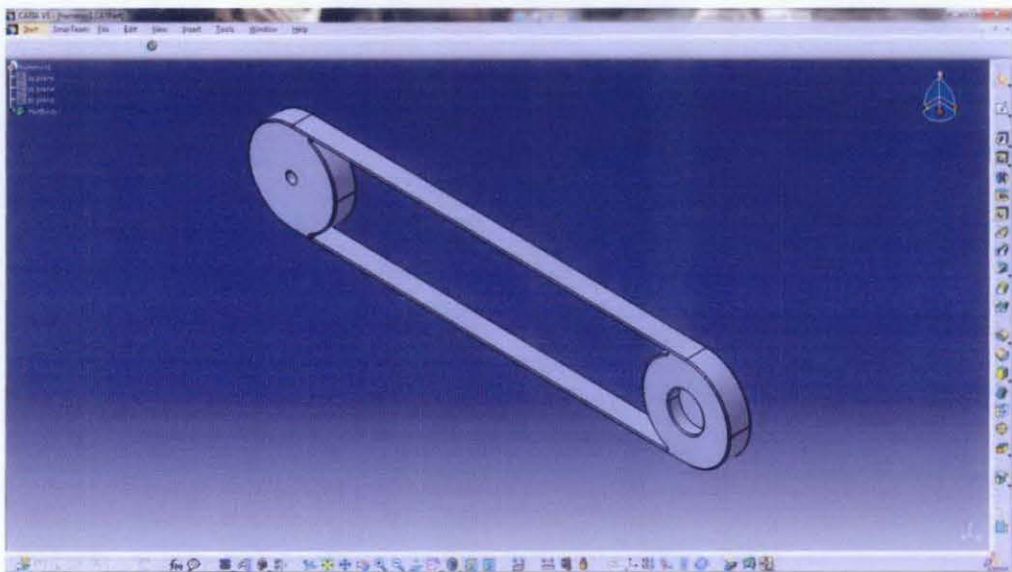


APPENDICEX B

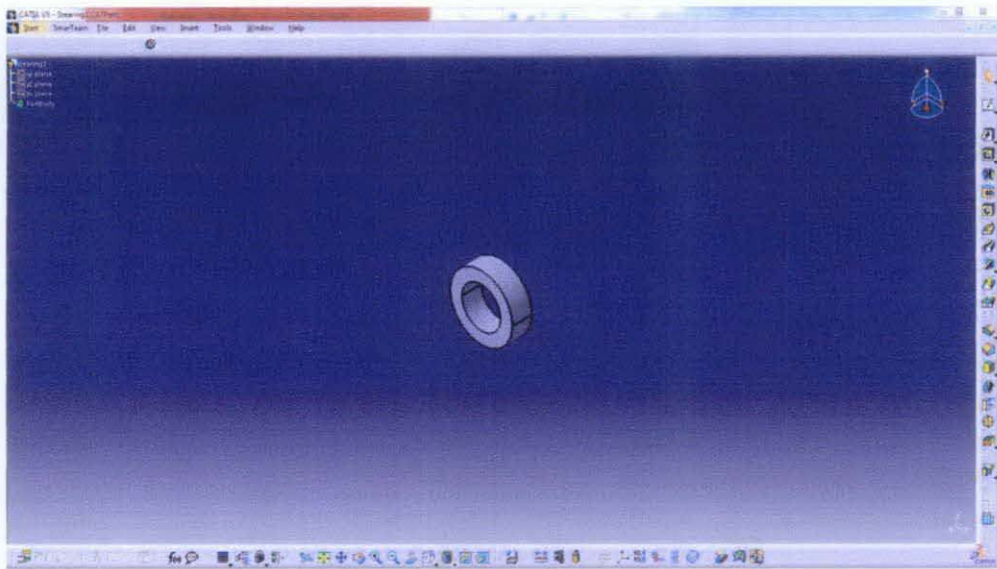
1. Isometric view of the artificial limb structure



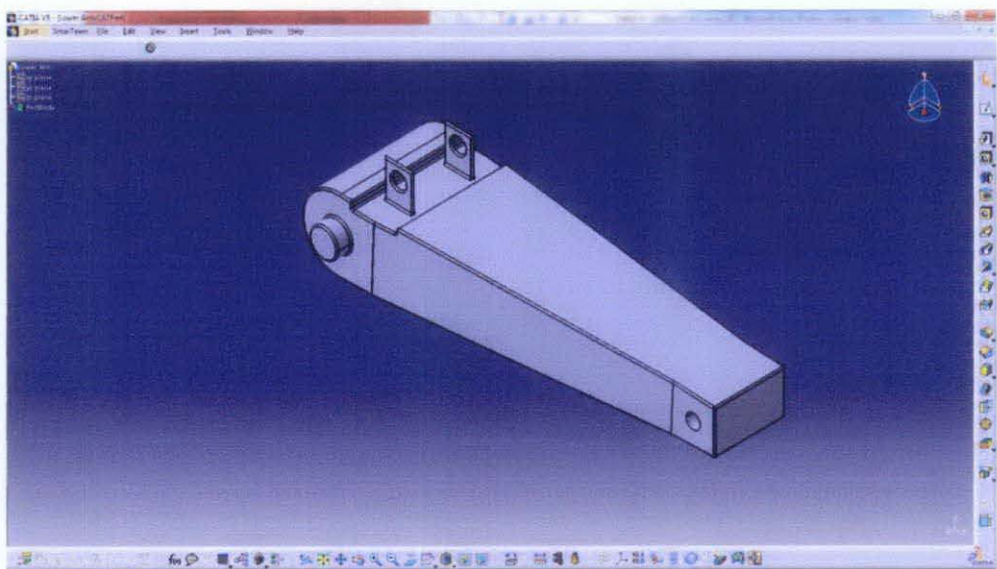
2. Isometric view of the Humerus (upper arm) of the limb structure



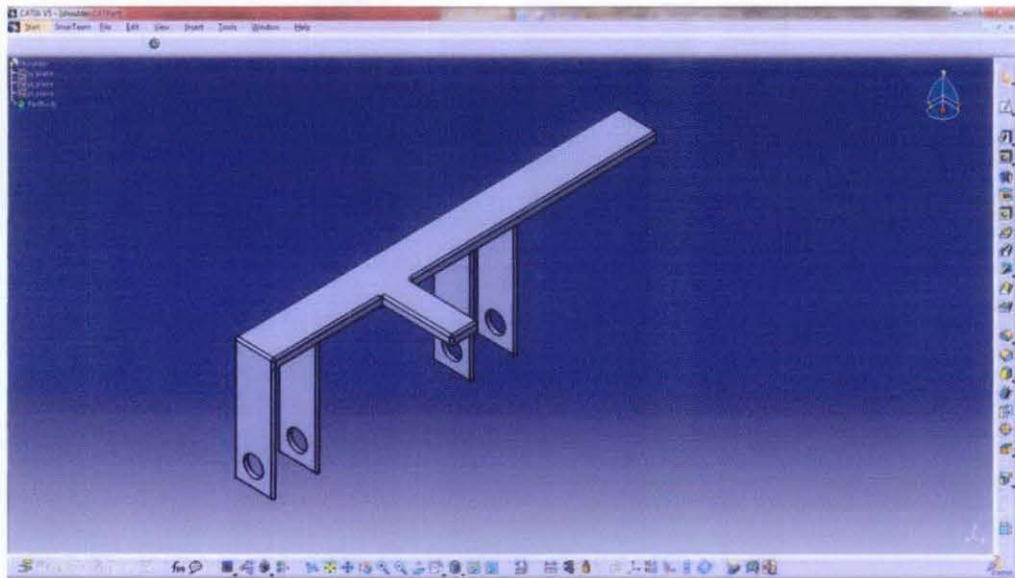
3. Isometric view of the Bearing



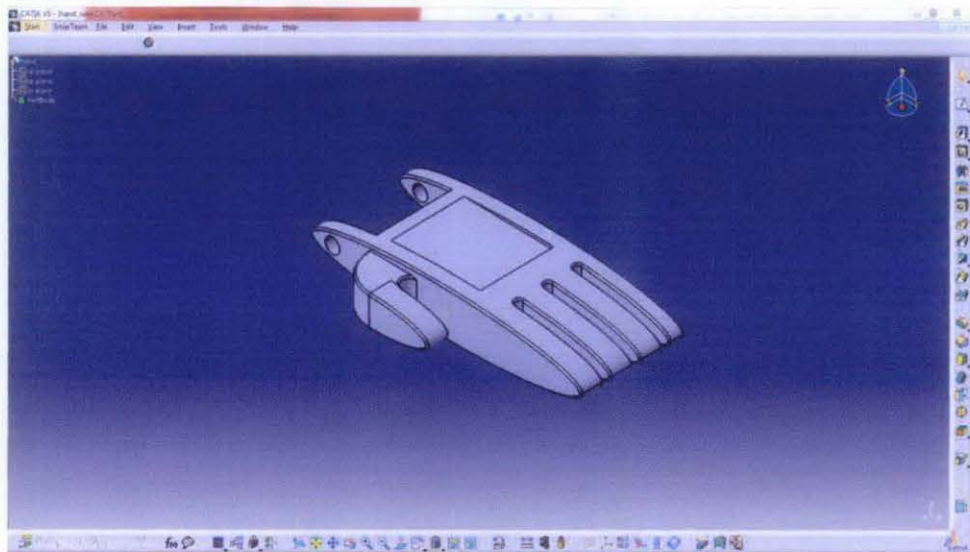
4. Isometric view of the Lower Arm



5. Isometric view of the Shoulder

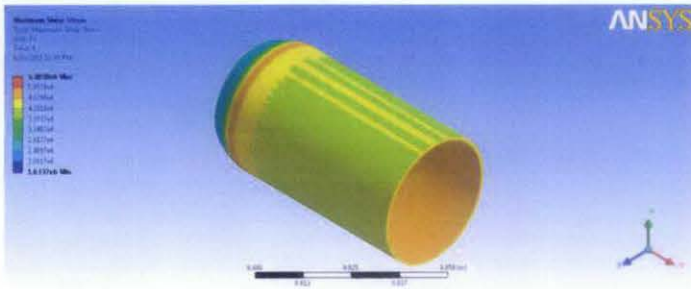


6. Isometric view of the Hand

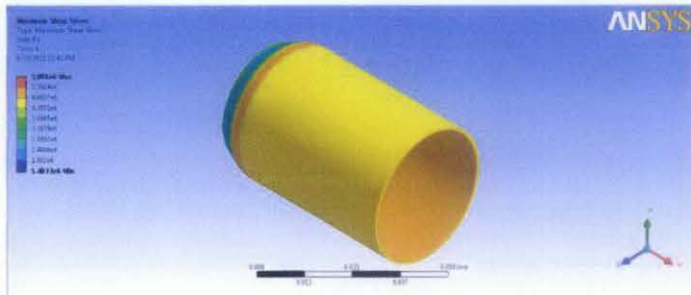


APPENDIX C

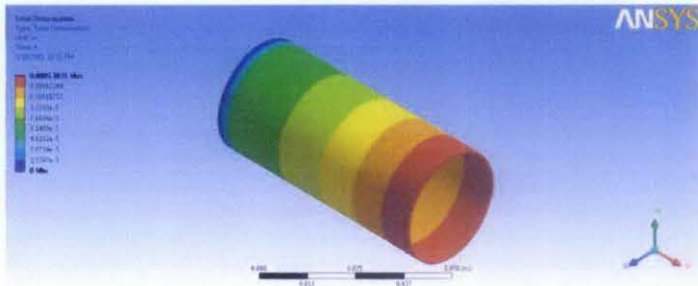
1. Shear stress for OD=30mm at $i=1$



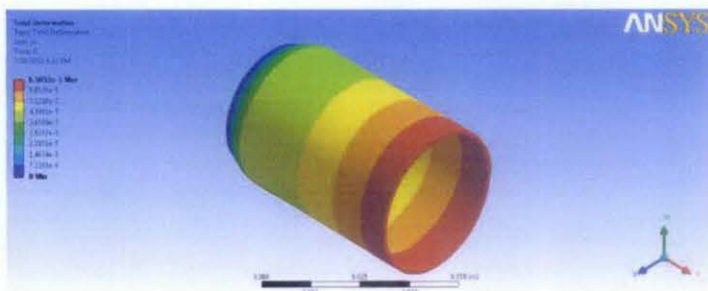
2. Shear stress for OD=30mm at $i=26$



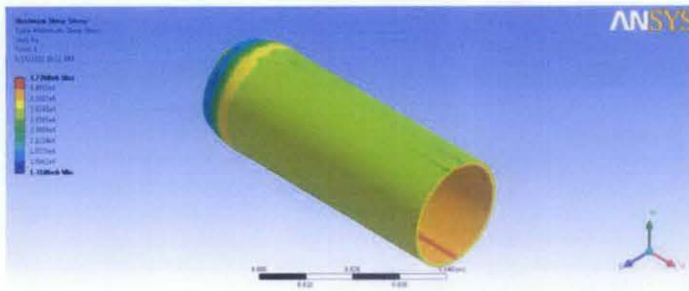
3. Total deformation for OD=30mm at $i=1$



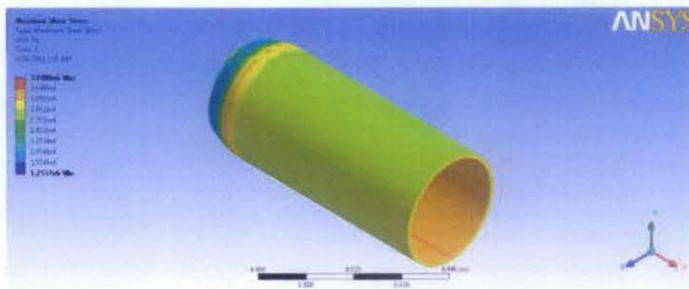
4. Total deformation for OD=30mm at $i=26$



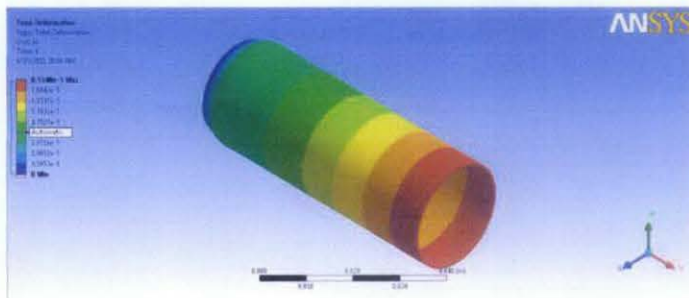
5. Shear stress for OD=20mm at $i=1$



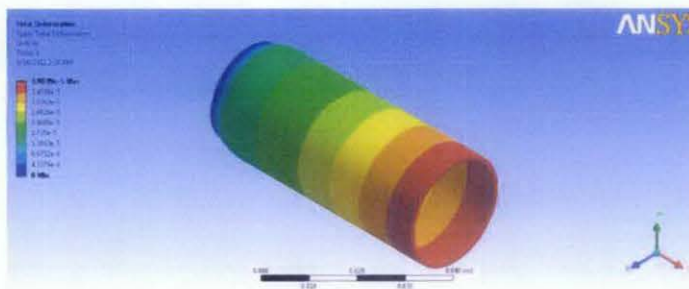
6. Shear stress for OD=20mm at $i=34$



7. Total deformation for OD=20mm at $i=1$

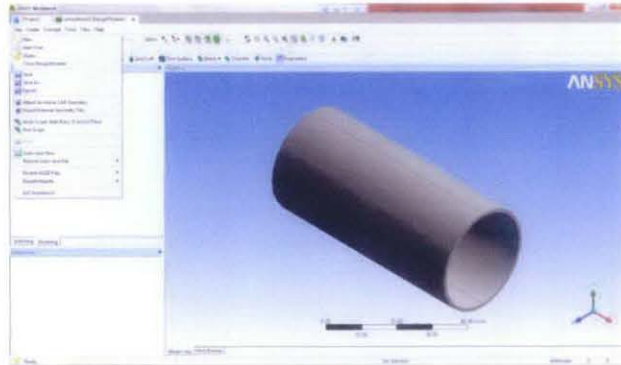


8. Total deformation for OD=20mm at $i=34$

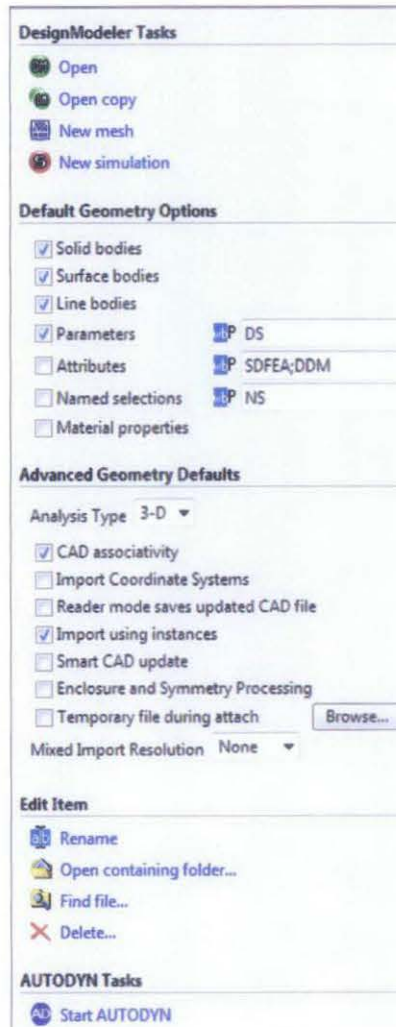


APPENDIX D

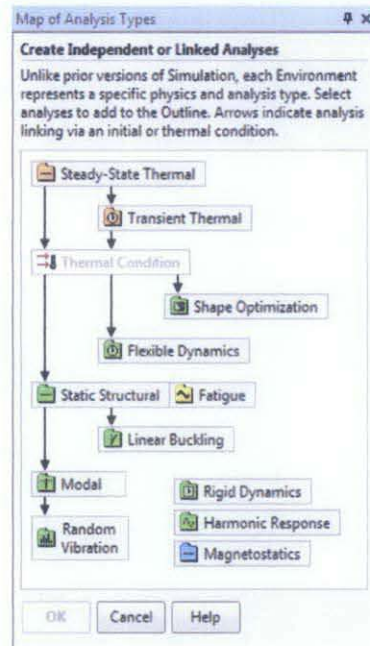
1. Import geometry from CATIA



2. New simulation



3. Create Static Structural Analysis



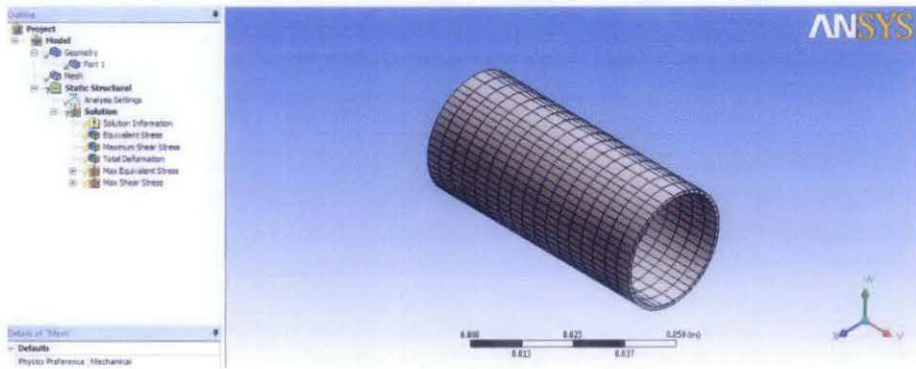
4. Engineering Data

Nylon	
Structural Add/Remove Properties	
<input type="checkbox"/> Young's Modulus	4.4e+009 Pa
<input type="checkbox"/> Poisson's Ratio	0.4
<input type="checkbox"/> Density	1200. kg/m ³
<input type="checkbox"/> Thermal Expansion	0. 1/°C
<input type="checkbox"/> Tensile Yield Strength	5.5e+007 Pa
Thermal Add/Remove Properties	
<input type="checkbox"/> Thermal Conductivity	0. W/m.*C
<input type="checkbox"/> Specific Heat	0. J/kg.*C
Electromagnetics Add/Remove Properties	
<input type="checkbox"/> Relative Permeability	0.
<input type="checkbox"/> Resistivity	0. Ohm-m

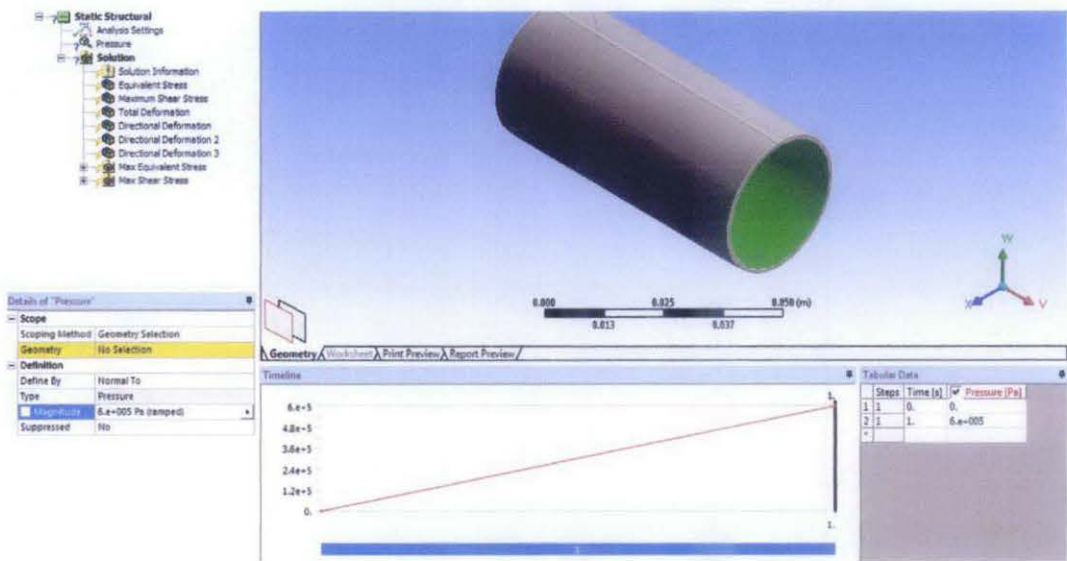
5. Details of the geometry

Details of "Part 1"	
Graphics Properties	
Definition	
<input type="checkbox"/> Suppressed	No
Material	Nylon
Stiffness Behavior	Flexible
Nonlinear Material Effects	Yes
Bounding Box	
Properties	
Statistics	

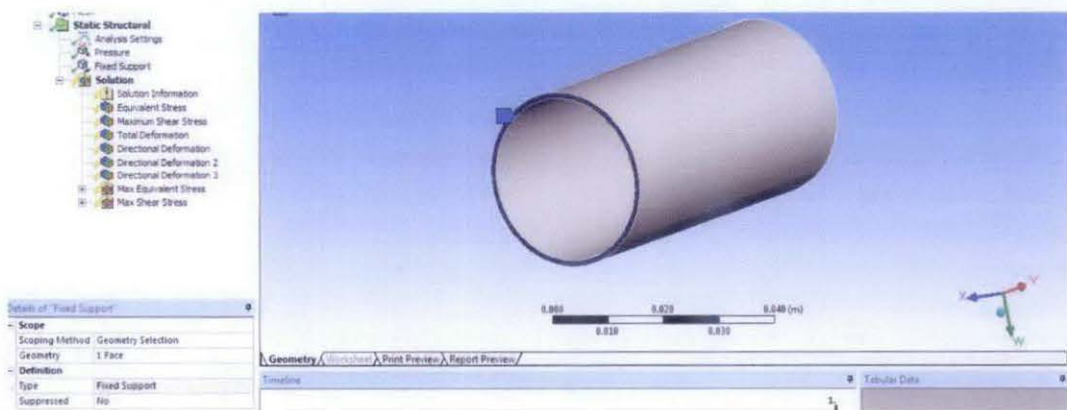
6. Meshing



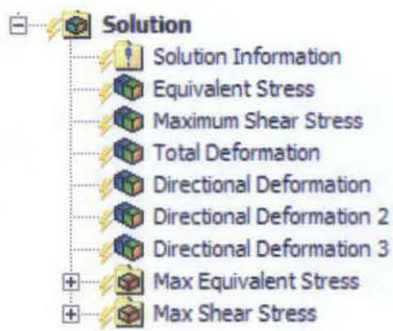
7. Insert pressure parameter



8. Insert fixed support parameter



9. Solution (output & result) parameters



10. Sample final results

